

Technical Report Documentation Page

1. Report No. FHWA/TX-89+1141-1	2. Government Accession No.	3. Recipient's Catalog No.	
4. Title and Subtitle The Use of Lasers for Pavement Crack Detection		5. Report Date December 1988	
		6. Performing Organization Code	
7. Author(s) Lynda Donnell Payne, Roger S. Walker		8. Performing Organization Report No. 1141-1	
9. Performing Organization Name and Address The University of Texas at Arlington Arlington, Texas 76019		10. Work Unit No. (TRAIS)	
		11. Contract or Grant No. Research Study # 8-18-89-1141	
12. Sponsoring Agency Name and Address Texas State Department of Highways and Public Transportation, D-10 Research P.O. Box 5051, Austin, Texas 78763		13. Type of Report and Period Covered Interim	
		14. Sponsoring Agency Code	
15. Supplementary Notes Study done in cooperation with US Dept. of Transportation, Federal Highway Administration			
16. Abstract This research was initiated to investigate the capability of using lasers for crack detection in pavements. If such a capability could be developed, it would be used to aid in obtaining and evaluating pavement distress and cracking information for the State's P.E.S. procedures, used for maintaining and evaluating pavements. The research effort has involved three stages. The first two stages were to determine the crack detection capabilities of the laser probes, used on the Surface Dynamics Profilometer (SDP). The SDP is owned by the State and used for road profile measurements. After experiments indicated that these probes could be used for such detection, a system was developed to further study this capability and to determine how it could be used to implement an automated high speed crack identification system. The third stage is the implementation of such a system so its usefulness for P.E.S. data collection activities can be determined. This research report describes the first two phases of the research effort.			
17. Key Words Surface Dynamics Profilometer (SDP) Lasers, Pavement Distress Measurements, Pavement Crack Identification and Recording.		18. Distribution Statement No restrictions. This document is available to the public through the National Technical Information Service, Springfield, Virginia 22161.	
19. Security Classif. (of this report) Unclassified	20. Security Classif. (of this page) Unclassified	21. No. of Pages 78	22. Price

THE USE OF LASERS FOR
PAVEMENT CRACK DETECTION

by

Lynda Donnell Payne
Roger S. Walker

The University of Texas at Arlington

Research Report 1141-1

Crack Identification Using Lasers

Research Project 8-18-88-1141

conducted for

Texas State Department of Highways
and Public Transportation

in cooperation with the
U.S. Department of Transportation
Federal Highway Administration

December 1988

The contents of this report reflect the views of the authors, who are responsible for the facts and accuracy of the data presented herein. The contents do not necessarily reflect the official views or policies of the Federal Highway Administration. This report does not constitute a standard, specification, or regulation.

There was no invention or discovery conceived or first actually reduced in the course of or under this contract, including any art, method, process, machine, manufacture, design or composition of matter, or any new and useful improvement thereof, or any variety of plant which is or may be patentable under the patent laws of the United States of America or any foreign country.

PREFACE

This project report presents interim results from Project 8-18-87-1141. The Project was initiated to determine the feasibility of using lasers for developing an automated pavement crack detection and identification system. This report provides results of the first two phases of the research effort.

Special recognition is due Mr. Robert Harris of D-18, for his support in initiating the project and his many contributions to this research efforts.

Lynda Donnell Payne
Roger S. Walker

December 1988

ABSTRACT

This research was initiated to investigate the capability of using lasers for crack detection in pavements. If such a capability could be developed it would be used to aid in obtaining and evaluating pavement distress and cracking information for the State's P.E.S. procedures, used for maintaining and evaluating pavements.

The research effort has involved three stages. The first two stages were to determine the crack detection capabilities of the laser probes, used on the Surface Dynamics Profilometer (SDP). The SDP is owned by the State and used for road profile measurements. After experiments indicated that these probes could be used for such detection, a system was developed to further study this capability and to determine how it could be used to implement an automated high speed crack identification system. The third stage is the implementation of such a system so its usefulness for P.E.S. data collection activities can be determined. This research report describes the first two phases of the research effort.

KEY WORDS: Surface Dynamics Profilometer (SDP), Lasers, Pavement Distress Measurements, Pavement Crack Identification and Recording.

SUMMARY

This project was initiated to determine the feasibility of using the laser probes on the Surface Dynamics Profilometer (SDP) owned by the State Department of Highways and Public Transportation (SDHPT), for crack detection and identification. If found feasible a system was then to be developed for use on the ARAN measurement vehicle, also owned by the State so it could be used to aid in pavement distress measurements. The SDP was selected for the initial testing and evaluation as it had existing on-board laser equipment.

The initial investigations proved that the lasers on the SDP could be used for crack detection. Based on this result, the study has proceeded in obtaining the necessary equipment and developing algorithms and software for implementing an automated crack measuring system which hopefully could be used to aid in PES.

This report discusses the first two phases of this project, determining the feasibility of crack detection using the laser, and obtaining and testing equipment so such a system could be implemented. During these first two phases the capabilities and limitations have been identified.

To date, it appears that a system can be developed with a limited capability for crack identification and reporting which could be useful for PES data collection activities. The third phase of development and implementation of the automated crack identification system is currently in progress.

IMPLEMENTATION STATEMENT

An automated and objective procedure for crack measurements and recording would provide a significant savings to the State during P.E.S. data collection procedures. It could be used in many other areas where statistical information regarding pavement cracking is desired.

TABLE OF CONTENTS

PREFACE	iii
ABSTRACT	iv
SUMMARY	v
IMPLEMENTATION STATEMENT	vi
LIST OF FIGURES	ix
CHAPTER	
I. INTRODUCTION	1
1.1 Project and Report Scope	1
1.2 Background	2
1.3 Project Phases	3
1.4 Distress Types	4
1.5 Project Requirements	7
II. FEASIBILITY	11
2.1 Sampling and Update Rates	11
2.2 Resolution, Noise, and Texture	11
2.3 Could Cracks Be Detected?	12
2.4 The Real-time Issue	13
2.5 Laser Problems and Limitations	17
III. CRACK IDENTIFICATION HARDWARE	18
3.1 Optocator	18
3.2 68000 DAQ Board	24
3.3 COMPAQ Portable III	24

IV. TIME AND FREQUENCY ANALYSIS TECHNIQUES	28
4.1 Time Series	28
4.2 Stochastic Process	29
4.3 Ergodicity and Stationarity	30
4.4 Statistical Estimates	31
4.5 Power Spectrum Estimation	32
4.6 Linear Parametric Modeling	33
V. ANALYSIS OF PAVEMENT CRACKING DATA	36
5.1 Introduction	36
5.2 Variance Method for Real-Time Crack Counting	36
5.3 Spectral Analysis Results	37
5.4 Running Mean/Slope Threshold Method	38
5.5 Autocorrelation Difference Method	41
5.6 AR Process Modeling Results	46
VI. CONCLUSIONS AND FURTHER RESEARCH	49
APPENDIX	
A. DAQ BOARD SCHEMATICS	52
B. RUNNING MEAN/SLOPE THRESHOLD LISTING	59
REFERENCES	65

LIST OF FIGURES

1.1	Rutting	5
1.2	Patching	5
1.3	Failure	6
1.4	Alligator cracking	6
1.5	Block cracking	8
1.6	Transverse cracking	8
1.7	Longitudinal cracking	9
2.1	Laser probe and laser calibration board	14
2.2	Laser orientations	15
2.3	Calibration board results	16
3.1	Laser probe and probe processing unit	19
3.2	Pulsed, modulated infrared light from GaAs lasers	21
3.3	Triangulation principle	22
3.4	Laser measurement range	23
3.5	CPU sub-rack with power supply and receiver-averaging boards	25
3.6	Data acquisition (DAQ) boards	27
3.7	Crack system in the profilometer	27
5.1	Power spectral density plots of different cracking types	39
5.2	Power spectral density plots of different cracking severity	40

5.3	Running mean/slope threshold technique applied to moderate alligator cracking data	42
5.4	Running mean/slope threshold technique applied to severe alligator cracking data	43
5.5	Raw data	45
5.6	Filtered data with $r(0)-r(4)$ value plotted every 16 data points	47
5.7	Actual $r(0)$ and $r(4)$ values for the data in Figure 5.6	48

CHAPTER I

INTRODUCTION

1.1 Project and Report Scope

This project was initiated to determine the feasibility of using the laser probes on the Surface Dynamics Profilometer (SDP) owned by the State Department of Highways and Public Transportation (SDHPT), for crack detection and identification. If found feasible a system was then to be developed for use on the ARAN measurement vehicle, also owned by the State. The SDP was selected for the initial testing and evaluation as it had existing on-board laser equipment.

As will be discussed initial evaluations proved that the lasers on the SDP could be used for crack detection. Based on this result, the study has proceeded in obtaining the necessary equipment and developing algorithms and software for implementing an automated crack measuring system for PES.

This report discusses the first two phases of this project, determining the feasibility of crack detection using the laser, and obtaining and testing equipment so such a system could be implemented.

The third phase of development and implementation of the automated crack identification system is currently in progress and will be reported on in a later report.

This introductory chapter will first provide a background and general understanding of the crack detection and identification problem. Further, it explains some necessary terms and describes the project requirements. Chapter two, then addresses the feasibility issue. It describes the work done to determine if pavement cracking could be detected with the lasers. The third chapter describes the hardware designed and built for initial evaluation of a crack detection system. Chapter four defines and explains the statistical and signal processing theory used in the crack identification algorithms.

Chapter five describes the different crack identification algorithms employed. This chapter also describes results of the data analysis on the test sections used in the study.

Chapter six describes additional research, much of which is being conducted in the third phase.

1.2 Background

The evaluation of pavement surface conditions of the nation's highways is of major interest to transportation engineers. The State has been using such information in conjunction with other data in an established procedure for determining the condition of the State's highway system. This information is essential in determining which roads should be worked on, and how much money is needed to complete the work.

The State currently evaluates pavement surface conditions by considering both road roughness and pavement distress. A measure of road roughness is readily obtained with existing instruments. Pavement distress information is more difficult to obtain as it requires visual evaluation. Currently, SDHPT personnel attend the annual Pavement Evaluation System (PES) Rater Training School and then disperse to their respective districts throughout the state to rate pavement surfaces by "walking" the roads. Obviously, this process is very tedious and time-consuming. Also, since so many people are involved in the evaluation, the ratings are often not repeatable. An automated measurement system is needed to simplify the process and to obtain more consistent measurements.

This research represents the first attempt by the SDHPT to automate the process. The research was made possible when laser probes were purchased for use on the Surface Dynamics Profilometer (SDP). The SDP is used by the Department to obtain road profile measurements. Two lasers, one in each wheel path, are used to measure distances from the bottom of a survey vehicle to the road surface. These distance measurements, along with vertical acceleration measurements from two accelerometers, are used to obtain the road profile by removing the effects of the vehicle suspension system [1,2,3].

The laser system discussed in this study is built by Selective Electronic Co. (Selcom) of Sweden. The device is called an optocator. The system's basic components are the laser probes and probe processing units, which are mounted under the van, and the CPU sub-rack containing the power supply and receiver-averaging boards, which are installed inside the van.

The optocator measures distances to a surface using laser probes. Each probe emits a small infrared light beam that strikes the surface to be measured. The reflected light is focused onto a position-sensitive detector in the laser probe allowing accurate distance measurements [5]. Further

explanation of the optocator and measuring principle will be provided in Chapter III.

Since the lasers were available, highway department engineers wanted to know if these lasers could help identify pavement cracking. The intent of this study was first to determine the feasibility of using the existing lasers of the SDP to identify pavement cracking. Then, if feasible, the work would be extended to design and implement a system which would identify the specified cracking patterns. Few operational systems for crack identification using laser probes have been reported in the literature. Most studies for such systems have used video data [6,7]. The research herein does not use an elaborate video camera system, only existing lasers.

1.3 Project Phases

As noted above, this study consisted of three phases and this report is concerned with the first two phases. First, the feasibility of using the existing laser probes on the SDP had to be investigated. This involved determining whether or not the resolution of the laser probes was sufficient to detect cracking patterns. Also, the measurement update rate had to be considered to determine if the laser could supply the necessary sampling rate for crack identification at highway speeds. Another item of interest was the real-time issue. That is, how much, if any, of the processing and analysis could be performed in real-time with the van moving at highway speeds? If real-time computation was not feasible, what procedures could be developed to collect data for later processing?

Phase two was to begin once it was determined that cracks could be detected using the laser probes. This phase would involve designing, testing and implementing both the hardware and software for a system which could be used for crack detection and identification.

Although it has been stated that phase one was first investigated followed by phase two, this was not exactly the case. Obviously, some of the issues in phase one could only be addressed if there existed hardware and software to obtain the cracking data. In actuality, the phases overlapped and some of the hardware and software developed will be changed later based on results obtained. By the same argument the success of such systems can only be determined by actual implementation.

1.4 Distress Types

This research is only concerned with distress types in asphalt surfaced pavements since this type of road surface represents the largest percentage of the highway system in Texas.

The distress types which are currently recorded by PES raters on asphalt pavements are rutting, patching, failures, alligator cracking, block cracking, transverse cracking, and longitudinal cracking [8]. Each type will be described here for completeness; however, not all types are considered in this research.

A rut is a surface depression in the wheel paths. Rutting stems from a permanent deformation in any of the pavement layers or subgrade. It is usually caused by consolidation or lateral movement of the materials due to traffic loads. Refer to Figure 1.1.

Patches, shown in Figure 1.2, are repairs made to pavement distress. The presence of patching indicates prior maintenance activity, and is thus used as a general measure of maintenance cost.

A failure is a localized section of pavement where the surface has been severely eroded, badly cracked, or depressed. Failures are important because they identify specific structural deficiencies which may pose safety hazards. See Figure 1.3.

Alligator cracking is a series of interconnecting cracks caused by fatigue failure of the asphalt surface under repeated traffic loading. The cracking initiates at the bottom of the asphalt surface where tensile stress and strain is highest under a wheel load. The cracks propagate to the surface initially as one or more longitudinal parallel cracks. After repeated traffic loading the cracks connect, forming polygon-shaped, sharp-angled pieces that develop a pattern resembling chicken wire or the skin of an alligator. The pieces are usually less than 1 foot on the longest side. Alligator cracking occurs only in areas that are subjected to repeated traffic loading. Refer to Figure 1.4.

Block cracking divides the asphalt surface into approximately rectangular pieces. The blocks range in size from approximately 1 foot square to 100 feet square. See Figure 1.5. Cracking into larger blocks are generally rated as longitudinal and transverse cracking. Block cracking is caused mainly by shrinkage of the asphalt concrete and daily temperature cycling. It is not load associated, although load can increase the severity of individual cracks. This type of



Figure 1.1 Rutting



Figure 1.2 Patching



Figure 1.3 Failure



Figure 1.4 Alligator cracking

distress differs from alligator cracking in that alligator cracks form smaller, many-sided pieces with sharp angles. Also unlike block cracks, alligator cracks are caused by repeated traffic loadings.

Transverse cracking, seen in Figure 1.6, consists of cracks or breaks which travel at right angles to the pavement centerline. Transverse cracks are usually caused by differential movement beneath the pavement surface. They may also be caused by surface shrinkage due to extreme temperature variations. Although transverse cracks may occur at any spacing, they will be only considered such for this research if they occur at distances greater than 10 feet apart. More closely spaced cracks are counted as either alligator or block. PES data and SDHPT experience suggests that this assumption will cause only a minor error in statewide PES sections.

Longitudinal cracks are parallel to the pavement's centerline or laydown direction. They may be caused by a poorly constructed paving lane joint, shrinkage of the surface due to low temperatures or hardening of the asphalt, or a problem with the subgrade. Refer to Figure 1.7 (Note the figure also has block cracking).

This research effort considered only three of the seven distress types described above. Specifically, alligator, block, and transverse cracking were to be considered. Some of the other distress types, particularly failures and longitudinal cracking, could cause the cracking pattern to be misclassified due to the nature of the sensors used and the method of observation. This should become clear from later discussions.

1.5 Project Requirements

As previously described, this study involved using the existing lasers to identify cracking patterns . One laser was to be mounted in each wheel path, and one in the middle. Obviously, little, or no information across the lane could be recorded to help in the identification. The laser data was to be recorded and analyzed in real-time at highway speeds if possible.

The type, severity and percent area of cracking was to be determined from the laser data obtained. Type refers to one of the three types previously mentioned (alligator, block, or transverse). Severity is determined by the width of the crack. Slight cracks are less than 1/8 inch, moderate are 1/8 to 1/4 inch and severe are greater than 1/4 inch wide. Also, the percent of the section with each type of crack was to be noted. In the case of transverse cracks, a count of the



Figure 1.5 Block cracking

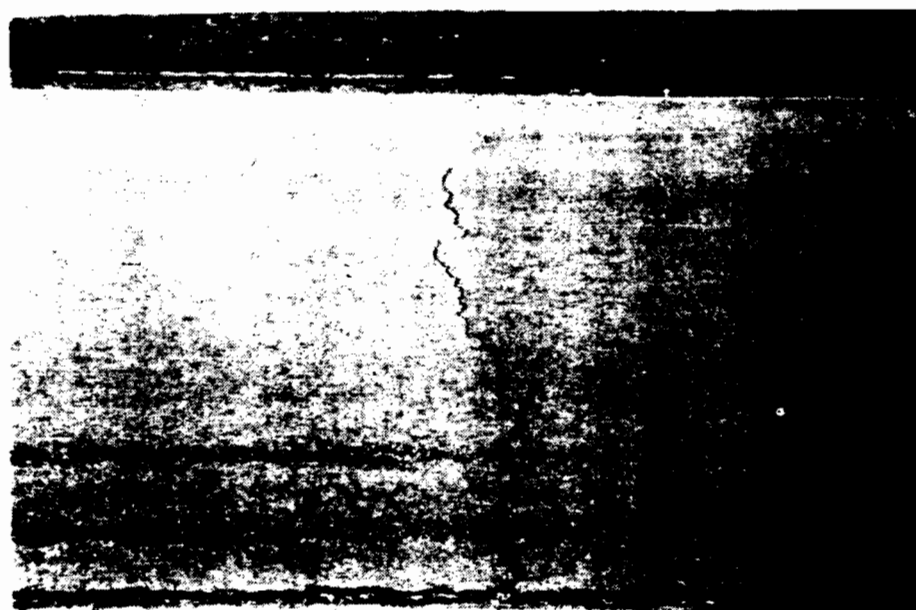


Figure 1.6 Transverse cracking



Figure 1.7 Longitudinal Cracking

number of cracks detected in a section length was to be reported.

Finally, if the complete data analysis and reporting could not be performed in real-time, then at least a reasonable (1 mile) length of data should be recorded in real-time. It could later be downloaded and further analysis and reporting performed.

CHAPTER II

FEASIBILITY

2.1 Sampling and Update Rates

The first question to be addressed in phase one was whether or not the lasers could provide measurements at a sufficiently fast rate. That is, did the laser update rate meet or exceed the necessary sampling rate? Since the smallest cracks to be detected were in the 1/8 inch wide range, it was reasonable that a 1/16 inch sampling rate would be required.

The update rate of the Selcom laser system is fixed with jumpers on the receiver-averaging board in the CPU sub-rack. This is discussed in Chapter III. However, the maximum update rate (no averaging) is 32,000 samples per second [4,5].

The necessary sampling rate for 1/16 inch sampling varies from 2816 samples per second at 10 miles per hour to 14080 samples per second at 50 miles per hour. A comparison of the update rate to the maximum required sampling rate shows that the Selcom lasers are able to supply measurements at the necessary speed. Also, since the update rate is more than twice the required sampling rate it is suggested that the receiver-averaging boards be jumpered for two point averaging. This will provide a 16K update rate, still exceeding the sampling rate required, and at the same time reducing the noise in the measurements.

2.2 Resolution, Noise, and Texture

The laser measurement range, as explained in Chapter III, is 10.04 inches. The analog signal from the laser probes varies from 0 to 10 volts. A 12-bit A/D converter in the probe processing unit (PPU) converts the analog signal into a 12-bit digital representation, providing a 2.44 mV or .00245 inch resolution.

Noise is a major consideration in determining measurement accuracy and the ability to detect cracking. That is, how much variability in measurement readings would be expected if the laser was reflecting off a surface at a constant distance?

To determine this the range and variance of two data sets was considered. In the first, the lasers were bench mounted in the lab and data was collected with the laser beam reflecting off a flat stationary object. Results from this procedure showed a range of + 28.9 to - 32.1 mV from the mean with a standard deviation of 7.9 mV.

A second set of data was collected in the profilometer with the motor running and the van at rest. Here the range was + 36.0 to - 37.2 mV from the mean and a standard deviation of 16.8 mV was observed. These observations were needed to provide insight into reasonable threshold values used in several of the crack detection algorithms.

The texture of a road surface is another item which adds variability. In fact, it should be understood that road surfaces of very coarse texture probably do not allow reasonable crack detection by the methods described in this study.

2.3 Could Cracks Be Detected?

Phase one of this project involved determining whether or not the Selcom lasers on the profilometer could detect cracks in a road surface. Two approaches were taken to answer this question. First, short sections of pavement with the desired cracking were located. The sections were marked as to start, end, and the desired path for the driver to take. Laser data was then obtained from the sections with the driver being very careful to follow the marked path. This data was plotted and compared with slides taken of the marked section. Results of this comparison were very encouraging. Most of the moderate and severe cracks seen in the slides could easily be recognized in the plots.

The first procedure of driving over a marked section gave a good idea but it was never known exactly where the laser beam fell. That is, a crack perpendicular to the centerline may be 1/4 inch wide at one point while 1/2 inch over it might be 1/16 of an inch wide. For this reason, that procedure did not give much insight into how well the lasers would be able to provide severity information. Therefore, a surface with cracks of known width and depth was needed for testing. To provide this known surface the laser calibration board was built.

The laser calibration board, though simple in concept and construction, provided valuable information. This board was simply a circular piece of black plywood suspended from a variable speed motor. Cracks of different widths and depths were cut into the board surface. The board was cut with a

desired circumference so it could easily simulate a road surface passing under the laser probes at speeds from 1 to 30 miles per hour by varying the rotational speed.

Three different sets of cracks were cut into the board. Cracks within each set were the same depth. That is, one set of cracks was 1/8 inch deep, one set was 1/4 inch, and the third set was 3/8 inch in depth. Five cracks of varying width were cut in each set. They were 1 inch, 1/2 inch, 1/4 inch, 1/8 inch, and 1/16 inch. Figure 2.1 shows the bench mounted laser probe, PPU, and the laser calibration board.

One important observation which came to light while working with the calibration board was that orientation significantly affected measurements. As will be discussed in Chapter III, the laser beam which strikes the measured surface is longer in one direction than the other. It was found that the ability to detect slight cracking was significantly improved by having the laser beam fall across a crack perpendicular to the centerline instead of into the crack. That is, orientation 2 in Figure 2.2 gave much better results. Also, orientation 1 gave invalid data readings on the back side of practically every crack. Invalid data is typically caused by an insufficient amount of laser light falling on the detector. Orientation 2 showed no invalid data. This observation can be explained by the fact that the entire beam fell into the crack in orientation 1 and the path of the reflected light back to the detector was obstructed by the crack wall as the beam neared the back side of the crack.

Figure 2.3 provides a plot of laser measurements obtained from the calibration board at 15 miles per hour using orientation 2. It can be seen that the 1 inch down to the 1/8 inch cracks are easily recognized. However, the 1/16 inch crack is not as easily detected. In fact, its true depth is not reflected in the plot. The reason is that the distance value represents the average distance measurement of all the area covered by the laser spot. Since the beam does not completely fall into the crack, the true depth of slight cracking cannot be accurately measured. This will cause a problem because slight cracking can easily be lost in the variability seen in noise and texture.

2.4 The Real-time Issue

The ability to detect and provide detailed analysis of pavement cracking at highway speeds up to 50 miles per hour cannot be performed by the hardware built in this initial study. Real-time analysis at speeds of 50 miles per hour with 1/16 inch sampling requires a processing time less than 71 microseconds.

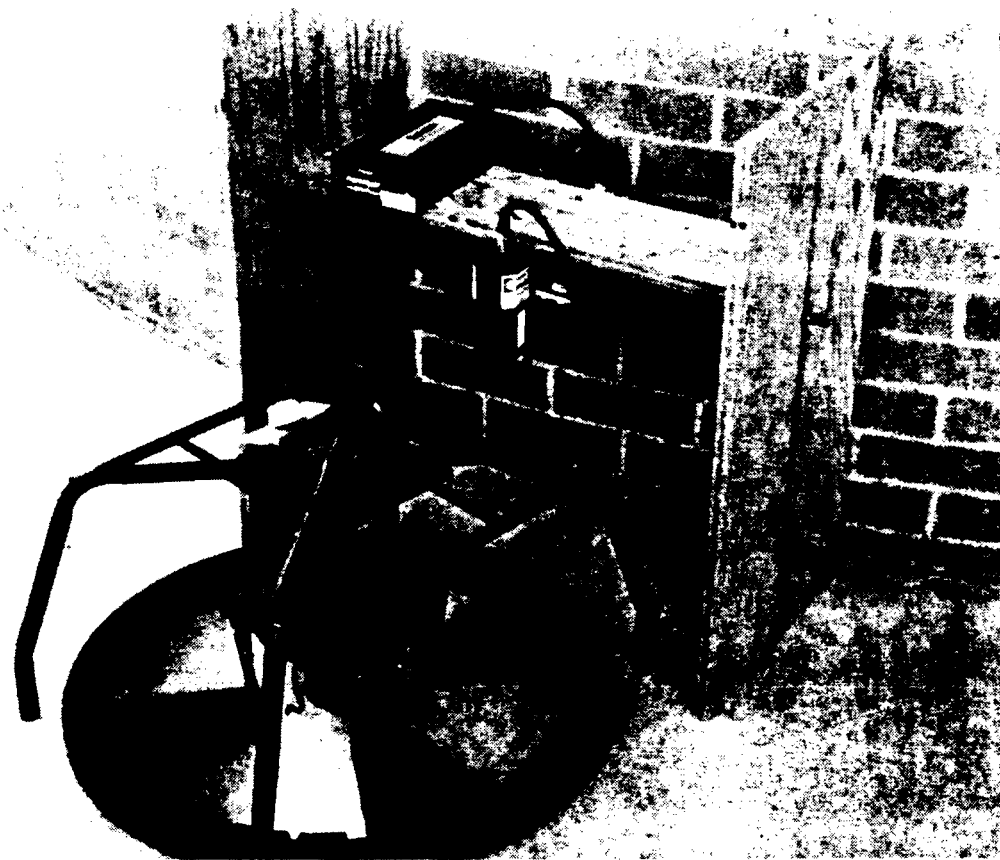


Figure 2.1 Laser probe and laser calibration board

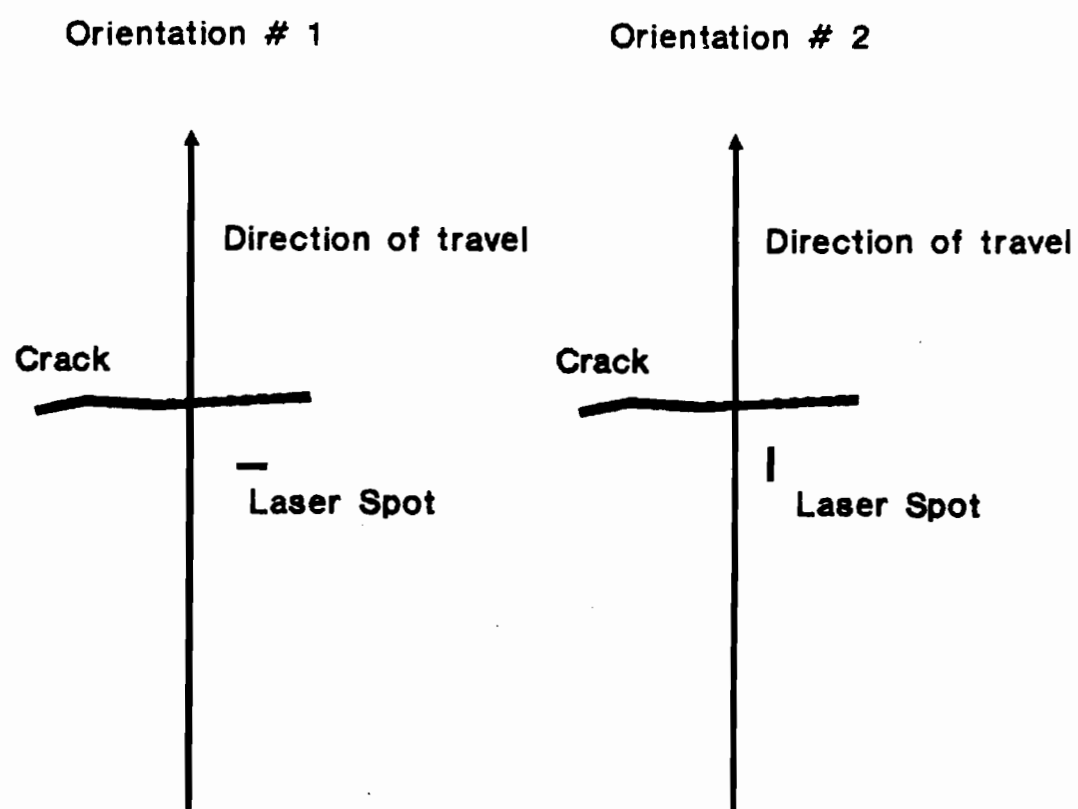


Figure 2.2 Laser orientations

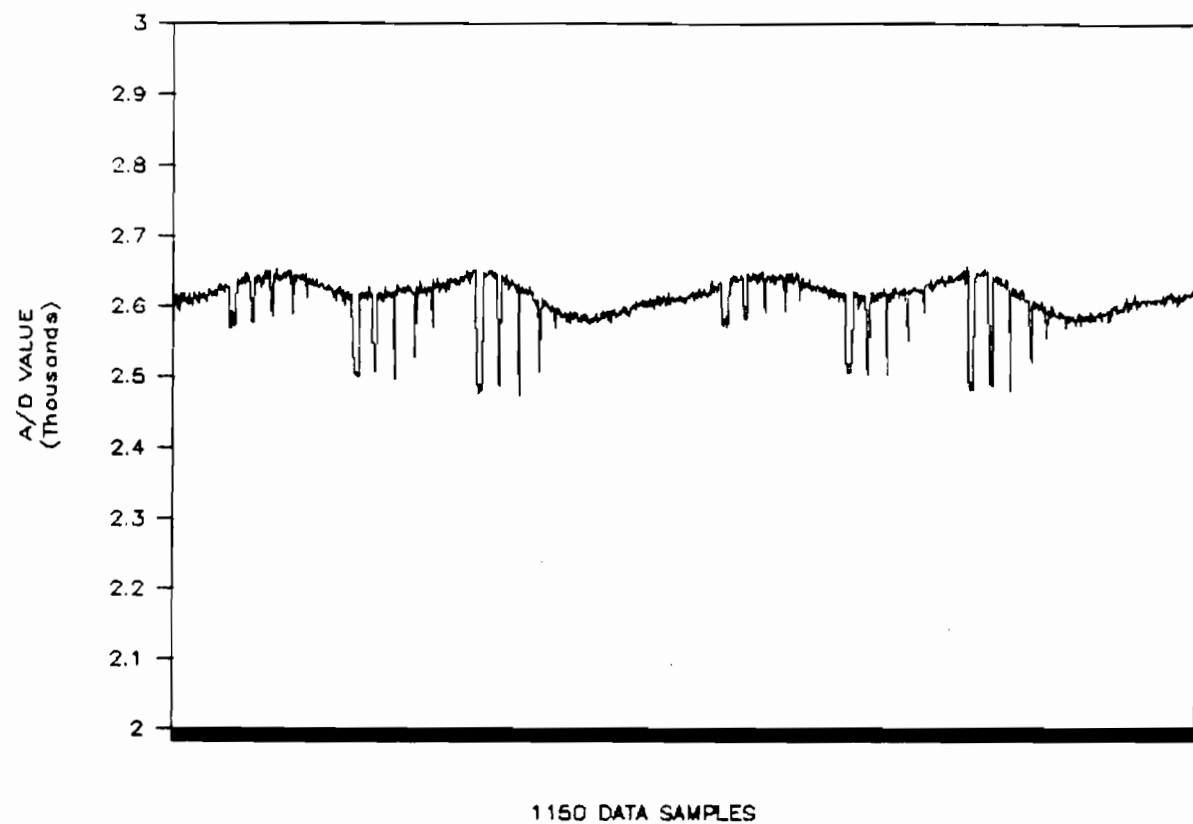


Figure 2.3 Calibration board results

Two revolutions of the calibration board are represented in the plot above. Note 3 sets of cracks with 5 cracks each are included in each revolution. Details of depth and width are described on page 17.

The system described in this study has the ability to give an approximate crack count in real-time or to collect a section of data in real-time which will later be downloaded, analyzed, and reported off-line. The real-time crack count feature is based on a variance calculation of one inch increments of data. These calculations can be performed in approximately 40 microseconds. It should be emphasized that this is only an estimate of cracking and is very sensitive to variance threshold values supplied by the operator.

Chapter VI will address the real-time issue again in a discussion of upgrades and further research.

2.5 Laser Problems and Limitations

Initial work in determining the sensitivity of the lasers to pavement cracking used the Selcom lasers installed in the profilometer. Based on results obtained from the calibration board experiments, a decision was made to obtain new lasers which had a reduced spot size. The laser probes with the larger spot size could not detect 1/16 inch cracking and even did a poor job of detecting 1/8 inch cracking. As expected, the new lasers did a much better job of detecting less severe cracks. Unfortunately, with the new laser system came many problems and delays.

The new lasers showed an abnormally high sensitivity to sunlight. In fact, results were so bad that the laser probes and probe processing units had to be sent back for modification. Following the modifications the probes were again bench tested both in the lab and outside in sunlight. Results obtained indoors or in a shaded area were acceptable; however, once again, when exposed to sunlight an abnormally high percentage of invalid data measurements were obtained.

Selcom technicians were again consulted. This time Selcom suggested changing the F-stop in the detector's lens system. To determine the best F-stop to use, data was collected from the laser calibration board in direct sunlight. Changing the F-stop from its preset 1.4 position to 4.0 seemed to eliminate the invalid data problem. The lasers were then field tested with mixed results. Sufficient data was collected to continue the study. Meanwhile, the laser probes and probe processing units were once again shipped back to Selcom for further modification and calibration.

It should be noted that Selcom engineers have since suggested not to change the F-stop more than two settings. They now recommend a setting of 2.8.

CHAPTER III

CRACK IDENTIFICATION SYSTEM HARDWARE

The three basic hardware components of the initial configuration for the crack identification system are the optocator, the 68000 DAQ board and the COMPAQ Portable III personal computer. The optocator obtains a distance measurement using non-contact lasers. The 68000 data acquisition board acquires the data from the optocator at a specified sampling rate, temporarily stores the data in onboard RAM and performs some preliminary processing of the data as well as data reduction. Finally, the COMPAQ accepts a reduced data set and stores it for final processing and analysis.

3.1 Optocator

The optocator is an optoelectronic measurement system which measures the distance to an object with high speed and precision. Most importantly, the measurement is made without contacting the measured surface. The basic components of the optocator are the non-contact laser probes, the probe processing units (PPU), and the CPU sub-rack which contains the power supply and the receiver-averaging boards which receive and process data from the gauge probes. A laser probe and probe processing unit are shown in Figure 3.1.

The gauge probe contains a pulsed, modulated (32KHz) and intensity-controlled laser diode, a position sensitive photodetector and an appropriate lens system. The laser diode is a class III b gallium-arsenide (GaAs) laser which entails the risk of eye damage if the beam hits the eye directly [4].

The GaAs laser in the gauge probe gives off pulsed, modulated invisible infrared light as shown in Figure 3.2. Each pulse in the 16 pulse burst is 350 ns. The bursts occur at a frequency of 32 KHz which accounts for the 32 KHz data rate of the serial data passed to the receiver-averaging board. The light from the laser beam passes through a lens which focuses the light in the center of the measurement range. The spot size which strikes the ground surface is approximately 1/4 inch by 1/16 inch.

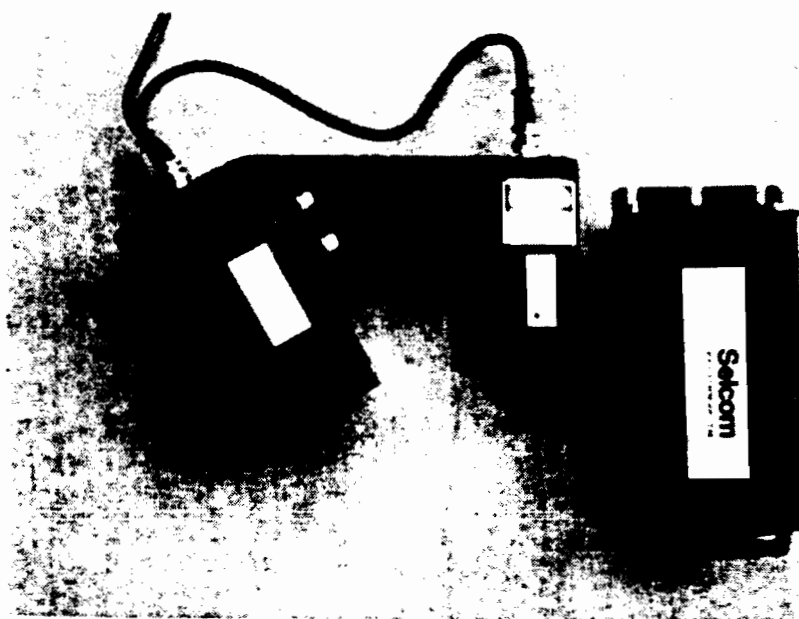


Figure 3.1 Laser probe and probe processing unit

The optocator measures the distance to an object by use of the triangulation principle, as illustrated in Figure 3.3. From a light source, L, a concentrated light beam is directed onto the surface of the measured object, O1. The light beam will strike the surface at point A and the scattered light reflection is focused through a lens to a point A' on a position sensitive detector. If the distance of the measured object is changed by X, the laser beam will hit point B on surface O2 and be focused at point B' on the detector. Since the relative position of the light source, the lens and the detector are fixed, the relation between X and X' is known and distance measurements can be obtained.

The maximum measurement range, O1-O2, as well as the standoff distance must be considered when mounting the laser probes. Selcom's gauge probe type 2008 requires a standoff distance of 355mm (13.98 inches) and has a measurement range of 256mm (10.08 inches) [5]. Therefore, to obtain correct measurements, the laser probes should be mounted such that the distance from the bottom of the probe to the ground surface (middle of the measurement range) is approximately 14 inches. When correctly mounted, distances plus or minus 128mm (5.04 inches) from the calibrated ground level can be accurately measured. Refer to Figure 3.4. Measured surfaces which do not fall within the measurement range will result in invalid readings.

The PPU processes the analog signal from the laser probe. It applies bandpass and anti aliasing filters to the signal. The PPU converts the analog signal into a serial digital form which can be transmitted over long distances to the receiver-averaging boards located in the CPU sub-rack. The serial digital output includes the 12 bit value from the analog to digital converter as well as 3 invalid data bits. The probe processing unit determines invalid data if the reflected laser beam is not correctly detected by the position sensitive detector in the probe. For example, if the measured surface is out of the measurement range, the invalid data bits would reflect this and the data could be processed accordingly.

Another function of the PPU is to control the intensity of the laser light emitted by the GaAs laser diode in the probe. This is done through a feedback mechanism.

The receiver-averaging boards are located in the CPU sub-rack as shown in Figure 3.5. There is one board for each laser probe. Each board receives serial data from the gauge probe at a rate of 32 KHz and is capable of reducing the data rate by forming the average of a number of measurements. The data rate, also referred to as updating frequency, is set by jumpers on the board. The update frequency ranges from a maximum of 32 KHz (no averaging) down to 62.5 Hz in powers of

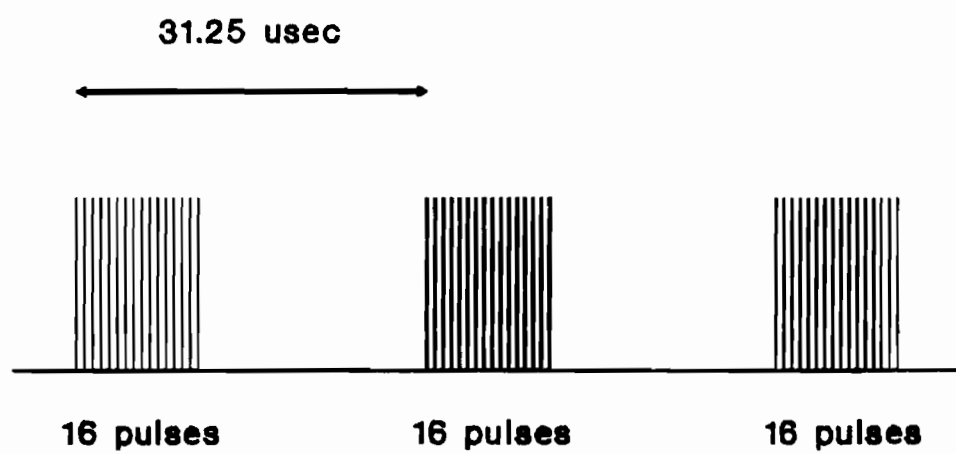


Figure 3.2 Pulsed, modulated infrared light from GaAs lasers

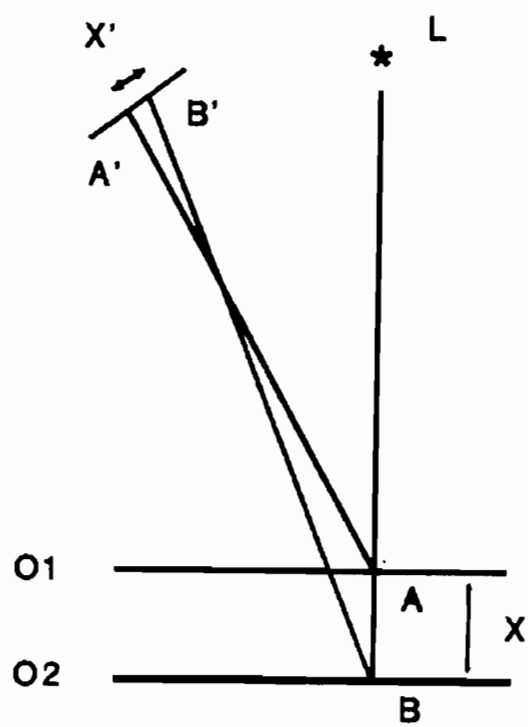


Figure 3.3 Triangulation principle

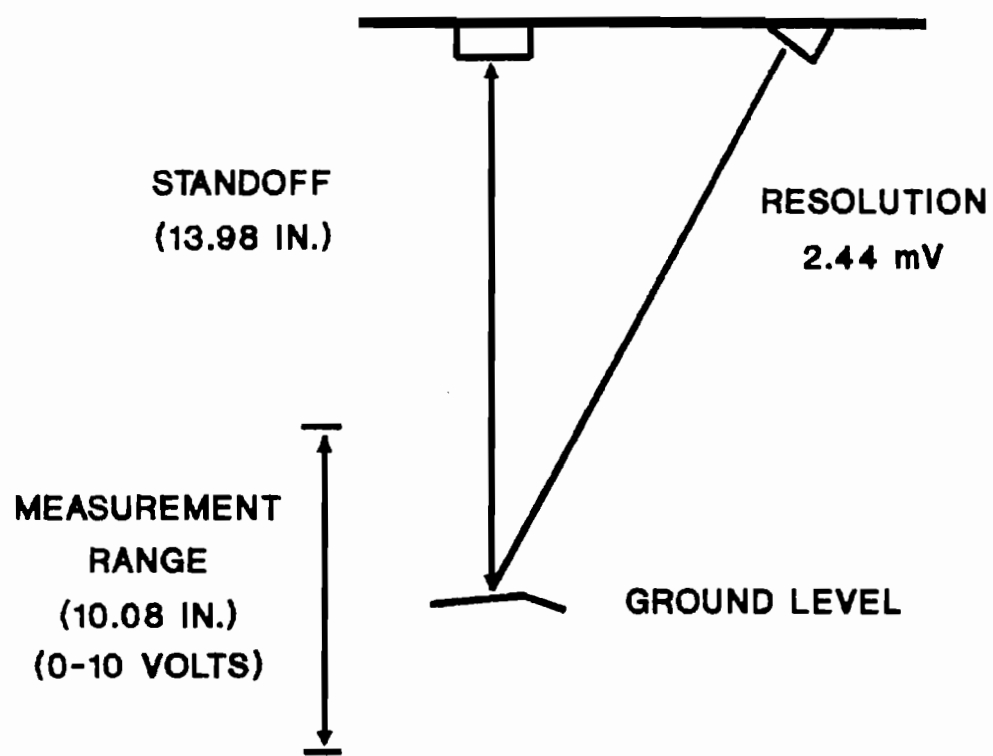


Figure 3.4 Laser measurement range

two.

Output from the receiver-averaging boards is the measured distance value represented as 12 bit parallel data plus a data invalid bit and a data ready flag. This 12 bit parallel data value is input to the 68000 data acquisition board (DAQ) which interfaces to the COMPAQ's PC bus.

3.2 68000 DAQ Board

The data acquisition board initially used to determine the measuring characteristics and capabilities for the project is a specially designed board which uses the Motorola 68000 processor and plugs into one of the system expansion slots in the COMPAQ Portable III expansion module (See Figure 3.6). Its function is to receive the laser data from the optocator and perform some preliminary processing of the crack data before passing it on to the COMPAQ Portable III for final crack identification and section analysis.

The DAQ board is actually made up of two boards. Schematics for the boards are included in Appendix A. The main board contains the M68000 microprocessor, static RAM, EPROM, serial and parallel I/O and is capable of running independently of the other. The second board is an auxiliary memory board which only contains buffers and an additional 512K of static RAM. This board is used when large amounts of data needs to be stored in real-time.

The main DAQ board features include an 8 MHz Motorola 68000 microprocessor, 64K static RAM, 64K EPROM, two Motorola 68230 parallel interface and timer chips, an Intel 8251 USART and the IBM PC interface.

The 8 MHz M68000 provides 500 nanosecond bus cycles. The static RAM and EPROMs have 100 and 200 nanosecond access time, respectively. This allows memory reads and writes with no wait states. The M68230 PI/T chips are programmed in the 16-bit port mode to provide the parallel interface for two lasers. The timers on the M68230 provide interrupt signals at the required sampling rate. The Intel 8251 USART gives an RS-232 compatible serial interface running at 9600 BAUD. The serial interface is used for most of the communications between the DAQ and the COMPAQ. The IBM PC interface provides an 8-bit parallel interface for downloading large amounts of laser data to the COMPAQ.

3.3 COMPAQ Portable III

The COMPAQ Portable III is the user's interface to the entire system. From the COMPAQ's keyboard the user can run diagnostic checks on the system, collect a specified amount of

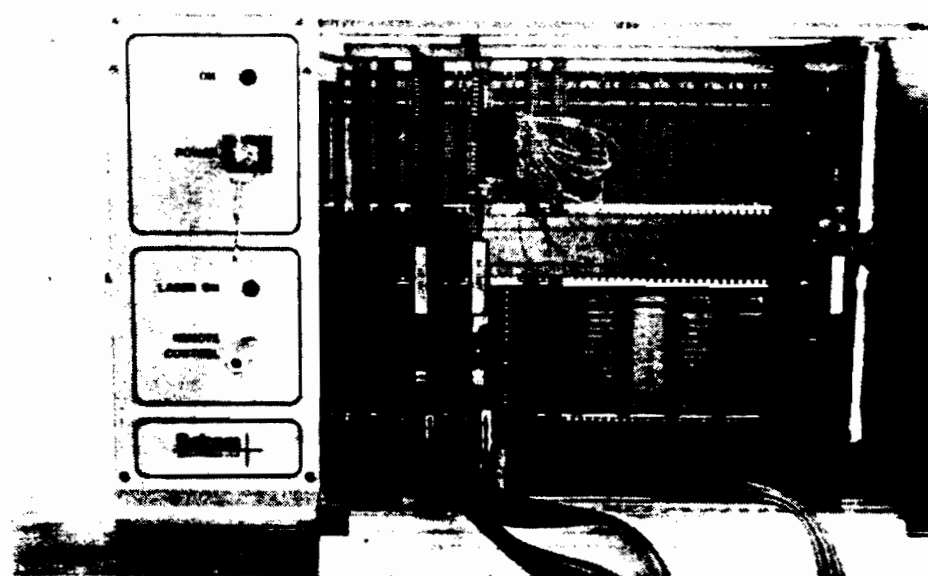


Figure 3.5 CPU sub-rack with power supply and receiver-averaging boards

data, download crack data to the COMPAQ for storage and subsequent processing, or enter a real-time crack counting mode.

The programs which provide detailed crack identification and section analysis reside on the COMPAQ. When the user runs a section of road to be analyzed, the data is collected on the DAQ boards and then downloaded to the COMPAQ for off-line analysis.

The real-time crack count mode provides a rough estimate of the number of cracks seen as the van moves at highway speeds. This estimate is performed by the DAQ board using a variance measure. In this mode the COMPAQ is used to issue the command to the system and to display the crack count.

Figure 3.7 shows the system as it is currently running in the profilometer.

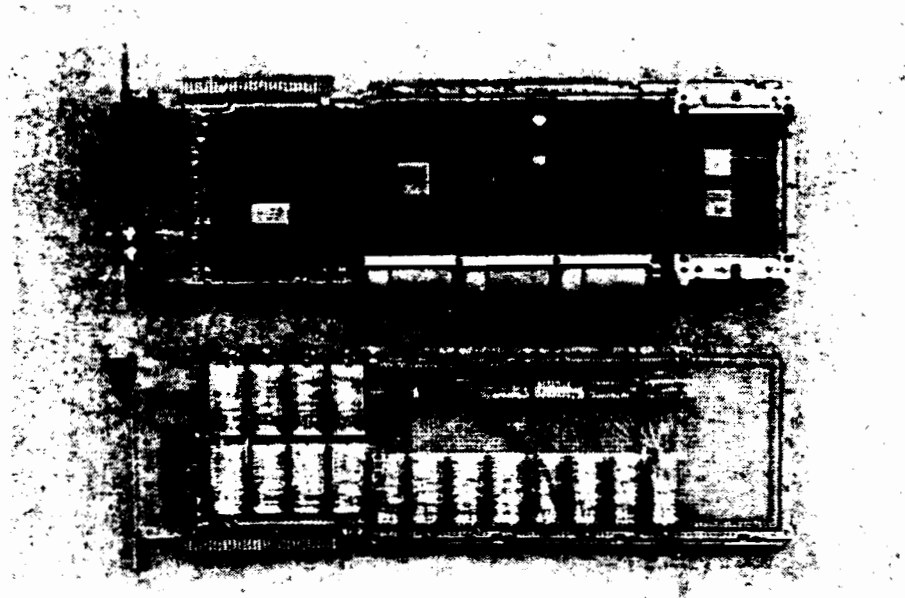


Figure 3.6 Data acquisition (DAQ) boards

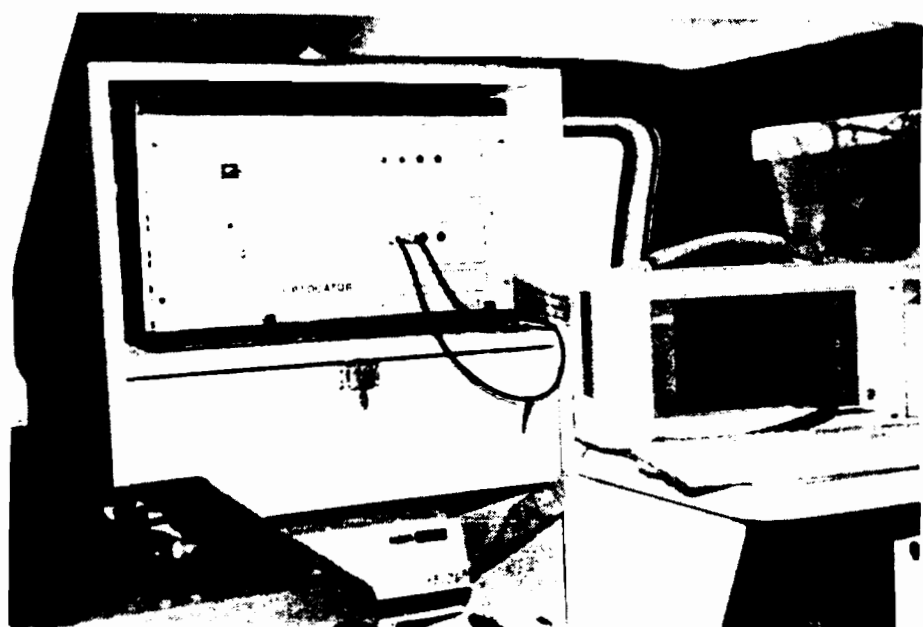


Figure 3.7 Crack system in the profilometer

CHAPTER IV

TIME AND FREQUENCY ANALYSIS TECHNIQUES

This chapter provides some of the basic concepts in the theory of time series analysis needed in the processing of crack data. Most important among these are the concept of a stochastic process, a stationary process, the autocovariance function of a stationary process, the frequency content of a time series, and linear parametric models. Several classical texts are included in the bibliography and may be referenced for a more detailed treatment of the subject [11,12,13].

It should be noted that all equations given in this chapter assume real-valued time series. Since complex-valued time series are not considered, the complex conjugation operator needed for the strictest definition of autocorrelation and autocovariance has been omitted.

4.1 Time Series

A signal which is continuous in time is a continuous time series. A discrete time series is simply a sequence of measurements or observations taken at specific instants of time. Often a discrete time series is a sampling of a continuous time series. Typically the observations are taken at equispaced time increments and denoted $x(n)$.

A continuous time series may be obtained by measurements taken from a physical instrument. Such a series is band-limited and contains no frequencies higher than the maximum frequency response of the measuring instrument. To analyze a continuous time series in discrete form the sampling interval must be determined such that all information present in the original signal is maintained. This sampling rate must equal or exceed twice the highest frequency present in the signal and is generally referred to as the Nyquist rate [14].

A signal from which the series was obtained could be deterministic or stochastic in nature. If it is possible to predict future values of the series exactly, the signal is deterministic. If future values can only be approximated based on statistical characteristics of past observations, the signal is a statistical or stochastic time series.

4.2 Stochastic Process

The possible values of the time series at a given time t are assumed to be described by a random variable $X(t)$ and its associated probability distribution. An observed value $x(t)$ at time t represents one of the infinite number of possible values of the random variable $X(t)$. The probability distribution function $F(x(t))$ defined by $F(x(t)) = \text{Prob}(X(t) \leq x(t))$ is the probability that random variable $X(t)$ has a value less than or equal to $x(t)$.

The behavior of the time series at all sampling times is described by an ordered set of random variables $\{X(t)\}$. The statistical properties of the time series are described by associating a probability distribution function with each random variable in the set. The ordered set of random variables $\{X(t)\}$ and the associated probability distribution functions is called a stochastic process. An observed time series $x(t)$ is only one of an infinite number of possible realizations of the stochastic process. The collection of all sequences that could result as realizations of the stochastic process is called an ensemble of sample sequences.

The expectation of a random variable $X(t)$ at time t , denoted by $E\{X\}$, is given by

$$E\{X\} = \int_{-\infty}^{\infty} x p(x) dx = \bar{x} .$$

Here x is the observation at time t and $p(x)$ is the probability density function of $X(t)$. This implies that the mean, \bar{x} , is based on values x taken from all possible ensembles of the random variable at time t .

The expected value of the squared magnitude of random variable X is

$$E\{|X|^2\} = \int_{-\infty}^{\infty} |x|^2 p(x) dx$$

is the mean squared value of X .

The variance of a random variable is the mean squared deviation of the random variable from its mean,

$$\begin{aligned}\text{var}(X) &= \int_{-\infty}^{\infty} |x - E(X)|^2 p(x) dx \\ &= E(|X|^2) - |E(X)|^2 .\end{aligned}$$

An indication of the statistical relationship of one random variable X_1 at time t_1 to another X_2 at time t_2 is given by the autocorrelation

$$r\{X_1X_2\} = E\{X_1X_2\} .$$

This represents the engineering definition for autocorrelation, as first suggested by Weiner. The autocorrelation of a stochastic process with the mean removed is the autocovariance, given by

$$\begin{aligned}c\{X_1X_2\} &= E\{(X_1 - E(X_1))(X_2 - E(X_2))\} \\ &= r\{X_1X_2\} - \bar{x}_1 \bar{x}_2 .\end{aligned}$$

If the random process has zero mean for time t_1 and t_2 then

$$c\{X_1X_2\} = r\{X_1X_2\}.$$

Also, if the random variables X_1 and X_2 are mutually independent or uncorrelated then

$$c\{X_1X_2\} = 0 .$$

This implies that there is no relationship between the two random variables and knowing values for X_1 does not help in predicting a value of X_2 .

4.3 Ergodicity and Stationarity

The definitions of mean, variance, autocorrelation, and autocovariance described above are based on statistical ensemble averaging. That is, they were based on observations at a particular time t . In practice one does not have the luxury of an ensemble of waveforms from which to evaluate these statistical descriptors. Typically these statistical

estimates are obtained from a single waveform $x(n)$ by substituting time averages for ensemble averages. Here $x(n)$ represents a discrete time series. For a stochastic process to be accurately described by time averages instead of ensemble averages the process must be ergodic. Ergodicity requires a certain amount of stationarity; that is, the statistics must be independent of the time origin selected.

A random process is wide sense stationary if its mean is constant for all time indices and its autocorrelation depends only on the time index difference m , where $m=n_2-n_1$. The variable m denotes the time lag, that is, the number of time increments between time n_2 and time n_1 .

All results reported in this study assume the data is wide sense stationary or at least locally stationary such that time averages can be substituted for ensemble averages.

4.4 Statistical Estimates

If a stochastic process is ergodic then

$$E\{X_1\} = E\{X_2\} = E\{X_3\} = \dots = E\{X_N\}$$

and the mean, \bar{x} , can be estimated by

$$\bar{x} = \frac{1}{N} \sum_{n=1}^N x(n) .$$

The autocorrelation and autocovariance functions no longer depend on the time index of the random variable, only the time index difference. The time index difference is referred to as the lag and denoted by m . The autocorrelation, r , and the autocovariance, c , then become

$$r(m) = E\{x(n+m) x(n)\}$$

and

$$\begin{aligned} c(m) &= E\{(x(n+m) - \bar{x})(x(n) - \bar{x})\} \\ &= r(m) - \bar{x}^2 . \end{aligned}$$

Assuming ergodicity, the autocorrelation and autocovariance can be estimated by

$$r(m) = 1/(N-m) \sum_{n=1}^{N-m} x(n) x(n+m)$$

and

$$c(m) = 1/(N-m) \sum_{n=1}^{N-m} (x(n) - \bar{x})(x(n+m) - \bar{x}) .$$

4.5 Power Spectrum Estimation

Spectral analysis is any signal processing method that characterizes the frequency content of a measured signal. In spectral analysis one is typically interested in obtaining a spectral plot which represents the distribution of signal strength at each frequency. Peaks in the spectral plot show which frequencies are predominant in the signal. Most power spectrum estimation is accomplished by either the autocorrelation or the direct method [15]. The latter method has become the most popular because of the fast Fourier transform (FFT) algorithm developed in 1965 [16]. The FFT is a fast, efficient algorithm for computing the discrete Fourier transform (DFT) of a time series. The DFT determines a sampled periodogram in which the values of the periodogram for only a discrete number of equally spaced frequencies is computed rather than evaluating over the continuous range of frequencies.

The method for calculating the power spectra in this study was first proposed by Welch [17]. This method segments the data, applies a window to each segment, determines the periodogram of each windowed segment, and then calculates the average periodogram, which is called the modified periodogram. With this method the data segments may be overlapped. This method of periodogram averaging reduces the variance of the spectral estimate.

The essential features of this method are described below. The available time series $x(n)$, $0 \leq n \leq N-1$, is divided into K overlapping segments of length L . The segments overlap by $L/2$ samples. The total number of segments then becomes

$$K = (N - L/2)/(L/2)$$

where any fractional portion of K is truncated. The i^{th} data segment then becomes

$$x_i(n) = x(iL/2 + n) w(n)$$

where $0 \leq n \leq L-1$, $0 \leq i \leq K-1$, and $w(n)$ is a window function of length L . Typically, either a rectangular or Hamming window is used.

The DFTs of each of the K data segments are then computed using the FFT algorithm by

$$X_i(k) = \sum_{n=0}^{M-1} x_i(n) \exp(-jkn(2\pi/M))$$

where $0 \leq k \leq M-1$ and $0 \leq i \leq K-1$. M is the DFT length and must be $\geq L$.

The modified periodograms, $S_i(k)$, are then averaged to produce the spectrum estimate

$$S(2\pi k/M) = 1/KU \sum_{i=0}^{K-1} S_i(k)$$

for $0 \leq k \leq M-1$, $0 \leq i \leq K-1$ and

$$S_i(k) = |X_i(k)|^2$$

and

$$U = \sum_{n=0}^{L-1} w^2(n)$$

4.6 Linear Parametric Modeling

Many discrete time stochastic processes can be approximated by a linear regression model. In this model, the input driving white noise series $w(n)$ and the observed output time series $x(n)$ are related by the linear difference equation

$$x(n) = b_0 w(n) + b_1 w(n-1) + \dots + b_q w(n-q) \\ - a_1 x(n-1) - \dots - a_p x(n-p) .$$

This may be rewritten in the form

$$x(n) = - \sum_{i=1}^p a_i x(n-i) + \sum_{i=0}^q b_i w(n-i) .$$

This general regression model is called an autoregressive-moving average (ARMA) model.

If all $a_i = 0$, then

$$x(n) = \sum_{i=0}^q b_i w(n-i)$$

and the process is known as a moving average model of order q and represented MA(q).

If all $b_i = 0$, $i > 0$, then

$$x(n) = - \sum_{i=1}^p a_i x(n-i) + b_0 w(n)$$

and the process is known as an autoregressive model of order p ; that is, AR(p).

Any one of the three parametric models described above may be expressed in terms of the other two models. An ARMA or MA model of a finite number of parameters may be described by an AR process, generally of infinite order. Similarly, an ARMA or AR process can be expressed as a MA model of infinite order. This observation is important because it suggests that any of the three models may be selected and a reasonable model obtained if a sufficiently large order is used. Of the three models, the AR model has mathematical characteristics which have allowed the development of a number of efficient algorithms. Specifically, AR models have linear solutions; whereas, solving for ARMA or MA parameters involves nonlinear equations.

Estimates of the AR parameters a_i can be obtained as solutions to the $p+1$ linear equations given by

$$\begin{bmatrix} r(0) & r(-1) & \dots & r(-p) \\ r(1) & r(0) & \dots & r(-p+1) \\ \vdots & \vdots & \ddots & \vdots \\ \vdots & \vdots & \ddots & \vdots \\ r(p) & r(p-1) & \dots & r(0) \end{bmatrix} \begin{bmatrix} 1 \\ a_1 \\ \vdots \\ \vdots \\ a_p \end{bmatrix} = \begin{bmatrix} |b_0|^2 \\ 0 \\ \vdots \\ \vdots \\ 0 \end{bmatrix}$$

These linear equations are commonly referred to as the Yule-Walker equations. The autocorrelation matrix is both Toeplitz and Hermitian because $r(-k) = r^*(k)$, where * represents complex conjugation. These properties allow more efficient solution than the standard Gaussian elimination. The method for solution of the Yule-Walker equations that takes advantage of these properties was developed by Levinson and is commonly referred to as the Levinson-Durbin algorithm [31,32].

CHAPTER V

ANALYSIS OF PAVEMENT CRACKING DATA

5.1 Introduction

The methods first investigated to identify pavement cracking are computationally intensive and cannot be performed in real-time with the hardware developed in this study. Each of these methods involve first filtering the data and then applying various statistical techniques to identify cracking. Data is filtered to remove the low frequency content of the signal. Low frequency components include such things as wheel bounce, vehicle suspension effects, bumps and hills in the section.

The two methods which consistently gave best results were the running mean/slope threshold technique and the autocorrelation difference method. These are discussed in detail in Sections 5.4 and 5.5, respectively. Another technique considered was modeling the data as an AR process and then examining the AR coefficients. This method would allow crack identification and classification if each cracking type would give distinctly different AR parameter values and the same type cracking would give similar coefficients. The AR modeling results are discussed in Section 5.6.

As stated, the methods mentioned above give detailed analysis and cannot be performed in real-time with existing hardware. It was desired to develop a technique, even a rough estimate, which could perform in real-time with the hardware described herein. A technique, using a variance measure, has been implemented which provides a crack count in real-time. This is discussed in the following section.

5.2 Variance Method for Real-Time Crack Counting

Although detailed crack identification and classification cannot be obtained using the DAQ board and COMPAQ at highway speeds, an estimate of the number of cracks seen is possible using a simple variance calculation. This method simply calculates the variance every 16 data points (1 inch) and compares that statistic to a threshold level provided by the operator. If the variance for that inch of data surpasses the

threshold, the count is incremented and displayed on the COMPAQ. This calculation takes approximately 40 microseconds on the DAQ board, well within the 71 microsecond requirement for 50 miles per hour.

The variance is calculated on 16 raw data values. Since unfiltered data is used, there exists variance in the data due to the factors previously mentioned which contribute to low frequency content of the signal. However, because only 16 data points are used in each calculation these components do not contribute as heavily to the variance value as high frequency cracks and thus filtering can be neglected to save calculation time.

The accuracy of this technique is highly dependent upon the operator entering meaningful threshold values. More investigation is needed to determine reasonable threshold limits for various pavement textures.

5.3 Spectral Analysis Results

Typically, one of the first things that should be considered about any measured signal is its frequency content. As previously discussed, spectral analysis provides this information. Of particular interest in this study was a determination of whether or not the different cracking types displayed characteristic power spectra. Also, it seemed reasonable that cracking of the different severity types might show characteristic peaks at different frequencies. The procedures described below provide information about the frequency content of pavement cracking data.

The first question addressed was whether or not each cracking type had its own characteristic spectrum. Here several data segments of 1000 data points in length were identified from the test sections for each of the desired types. The types considered were moderate alligator, moderate block, and no cracking. Moderate transverse cracking was not included because by using 1000 data points (5.2 feet) a single crack may or may not have been seen in the data; thus, it would appear as block or no cracking. A typical power spectrum for these three types is shown in Figure 5.1. Three important observations can be made from that figure.

First, no cracking appears as virtually a straight line. There are no frequencies or range of frequencies which are predominant. A flat power spectrum indicates white noise; that is, the signal is completely random and there is no correlation in the data. A second observation is that data with cracking shows no noticeable peaks at any frequencies but does consistently show more power at the lower frequencies (greater than 1/4 inch wavelengths). This suggests that data

with cracking is correlated and statistical measures such as autocorrelation and autocovariance will be appropriate. Finally, moderate alligator shows more power than moderate block at the low frequencies. This implies that more cracking means more correlation of the data and larger autocorrelation and autocovariance values should be observed.

Figure 5.2 shows typical power spectral results for sections with moderate versus severe alligator cracking. Initially it was felt that perhaps different severity (widths) of cracking might show peaks at different frequencies. This has not been observed. However, consistent with previous results, a higher degree of cracking again shows more power at wavelengths less than 1/4 inch. Slight alligator cracking was not included because it is not believed that the lasers are accurately measuring slight (less than 1/8 inch) cracks.

In summary, the spectral analysis results indicate that data obtained from road pavements with no cracking is uncorrelated. Data from pavement with cracking is correlated; in fact, the higher the degree and severity of cracking, the more correlated the data is.

5.4 Running Mean/Slope Threshold Method

The basic idea behind this method is that a running mean, representing ground level, is maintained and each new data value is compared with this mean to determine if it is a value taken from a crack or not. The term running is used because the mean must be constantly updated using the new data points to maintain an accurate representation of ground level. Data points which are determined to represent a crack or a surface too much above ground level, perhaps an extraneous rock or spikes in the data, do not contribute to the running mean calculation. The running mean is an average calculated from the last N data points which have been determined to be at ground level. N is user selectable, typically 4 to 8.

The simplest way to apply this technique is simply to compare each new data value to the running mean. If it is below a threshold distance from ground level then identify it as a crack, do not include it in the mean, and advance to the next point. If it is less than a threshold distance below the running mean then it is not a crack and the value replaces the "oldest" value used in the mean calculation and a new running mean is determined. Unfortunately this will not provide accurate crack identification for cracks with gently sloping walls. The problem is that although the values are decreasing they may not exceed the threshold using the technique described above and so they are included in the running mean. This lowers the mean value and makes it even more difficult for the next point to be identified as part of a crack. The

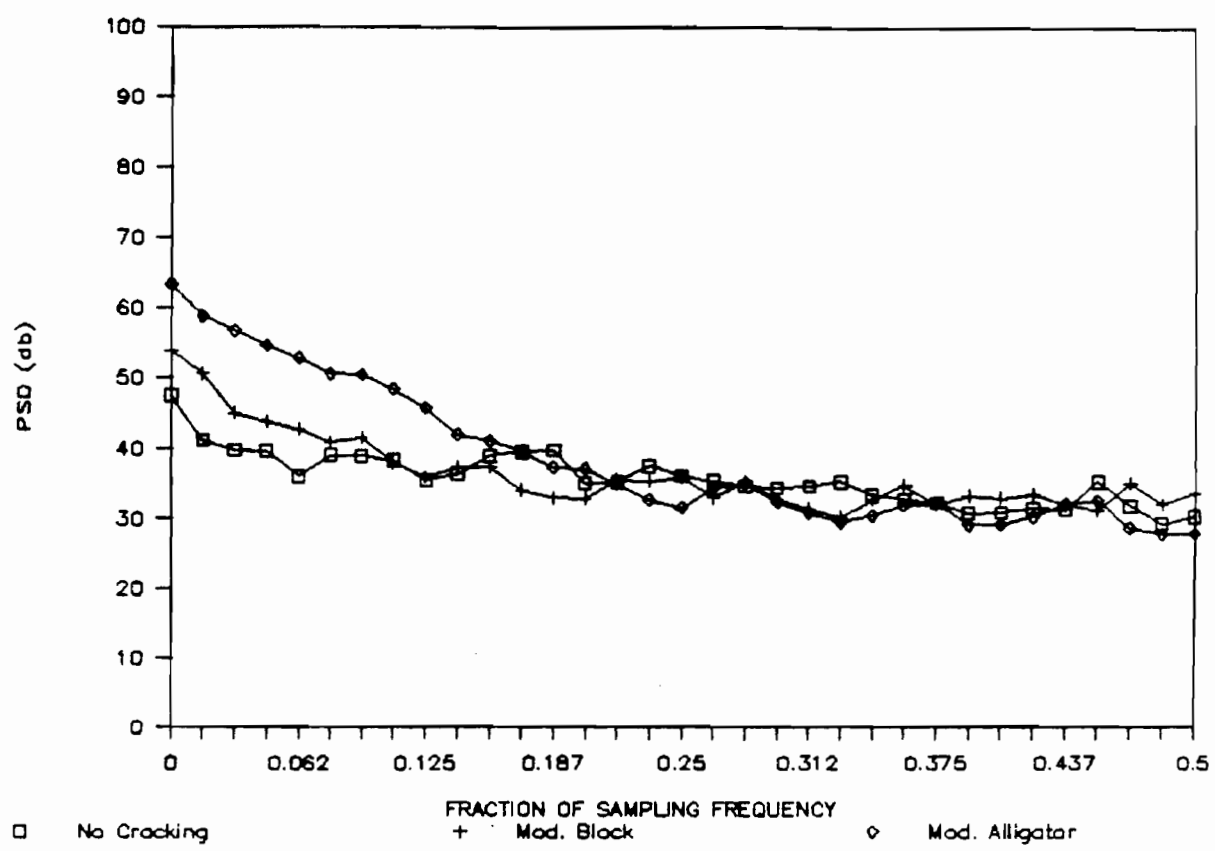


Figure 5.1 Power spectral density plots of different cracking types

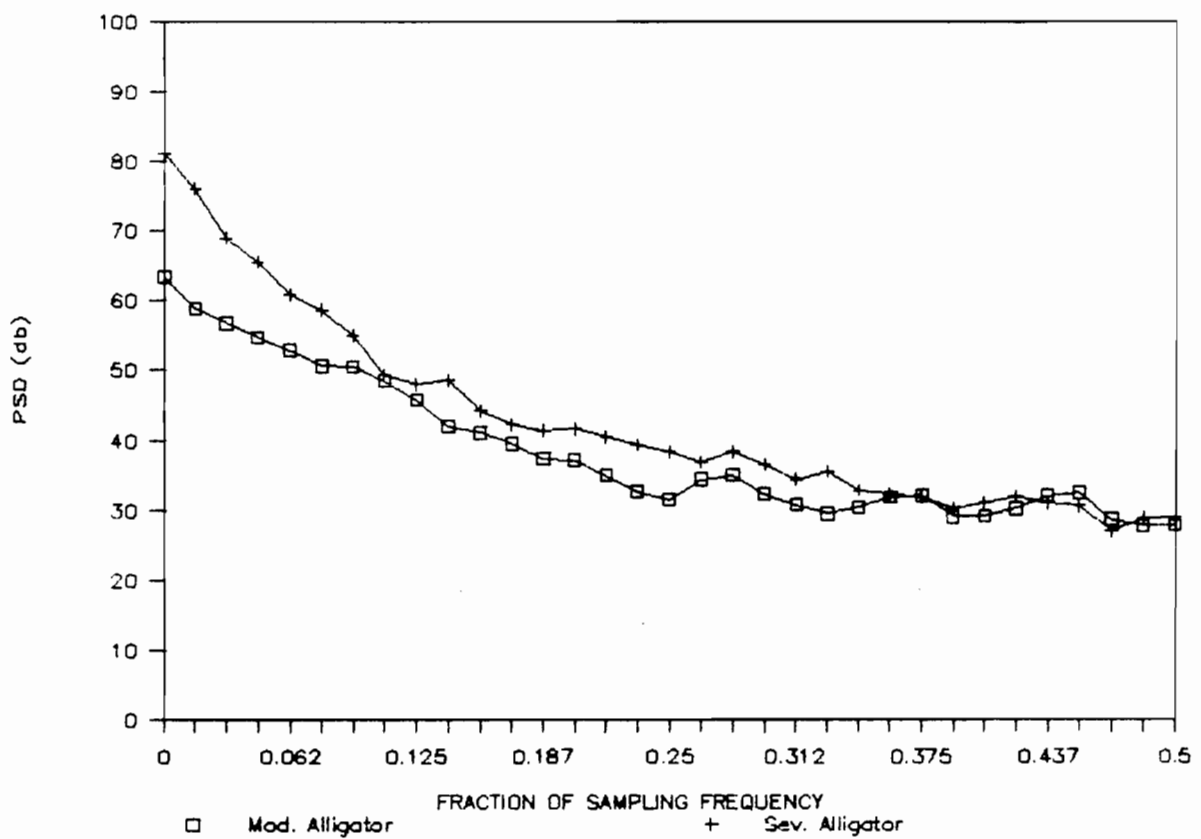


Figure 5.2 Power spectral density plots of different cracking severity

problem is solved by looking ahead up to L lookahead points, assuming all values are constantly below the mean, for a value exceeding the threshold before updating the running mean. L is a user supplied parameter. If the threshold is exceeded within L points, then each of the decreasing data points are identified as part of a crack and will not be included in the mean.

The accuracy of this method depends on the number of data points used in the mean, the number of data points allowed in the lookahead for threshold violation, and the threshold value itself. After plotting and examining results from various types of cracking in the test sections, it is believed that about 85% of the cracking can be identified using 4 points for the mean and lookahead value and 35 for a threshold level.

This technique performs better if the data is first filtered to remove the DC component and longer wavelengths. A highpass Butterworth filter is typically applied to the raw data.

Figures 5.3 and 5.4 show the results of applying this algorithm to moderate and severe alligator cracking, respectively. 1000 (5.2 feet) filtered data points have been plotted in both figures. Above the filtered data is a plot representing whether or not a crack has been seen. Ground level is plotted at 200 on the Y-axis and cracks at 100.

The running mean/slope threshold algorithm is included in Appendix B.

5.5 Autocorrelation Difference Method

The autocorrelation is a statistic which measures the correlation of data at different time increments apart. Assuming ergodicity, the autocorrelation lag m, denoted $r(m)$, tells if data points m time increments apart over a length of data are related. The autocorrelation value will be approximately zero if the data is uncorrelated. As shown by the power spectral analysis results of Section 5.3, data with cracking is correlated. Data with sharp cracks will show large correlation for a lag or two but the autocorrelation value decreases rapidly as the number of lags increases. Data with longer wavelength components, such as bumps, show high autocorrelation values for longer lag times.

Section 5.2 discussed a "quick and dirty" way of identifying cracks in unfiltered data by calculating the variance, $c(0)$, every 16 data points and then comparing that value to a threshold. That method was, at best, an estimate. However, because the data was not filtered and only a simple variance calculation was needed, it did meet the real-time

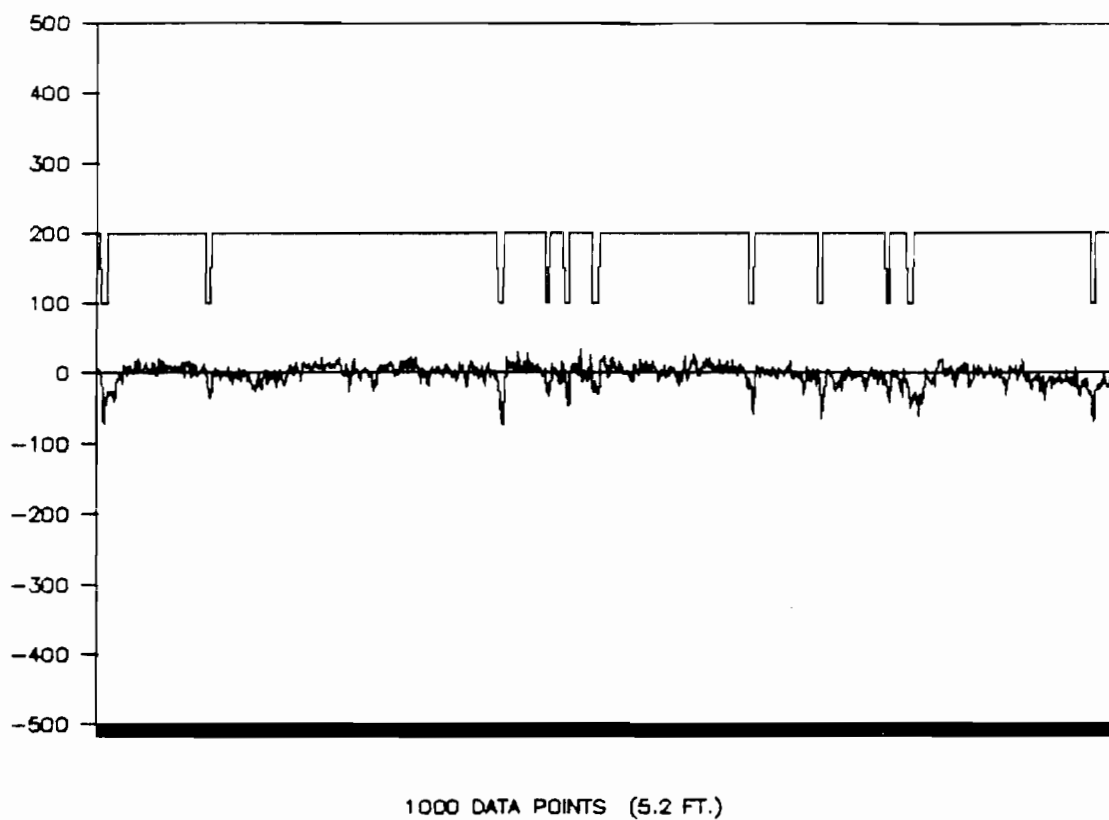


Figure 5.3 Running mean/slope threshold technique applied to moderate alligator cracking data

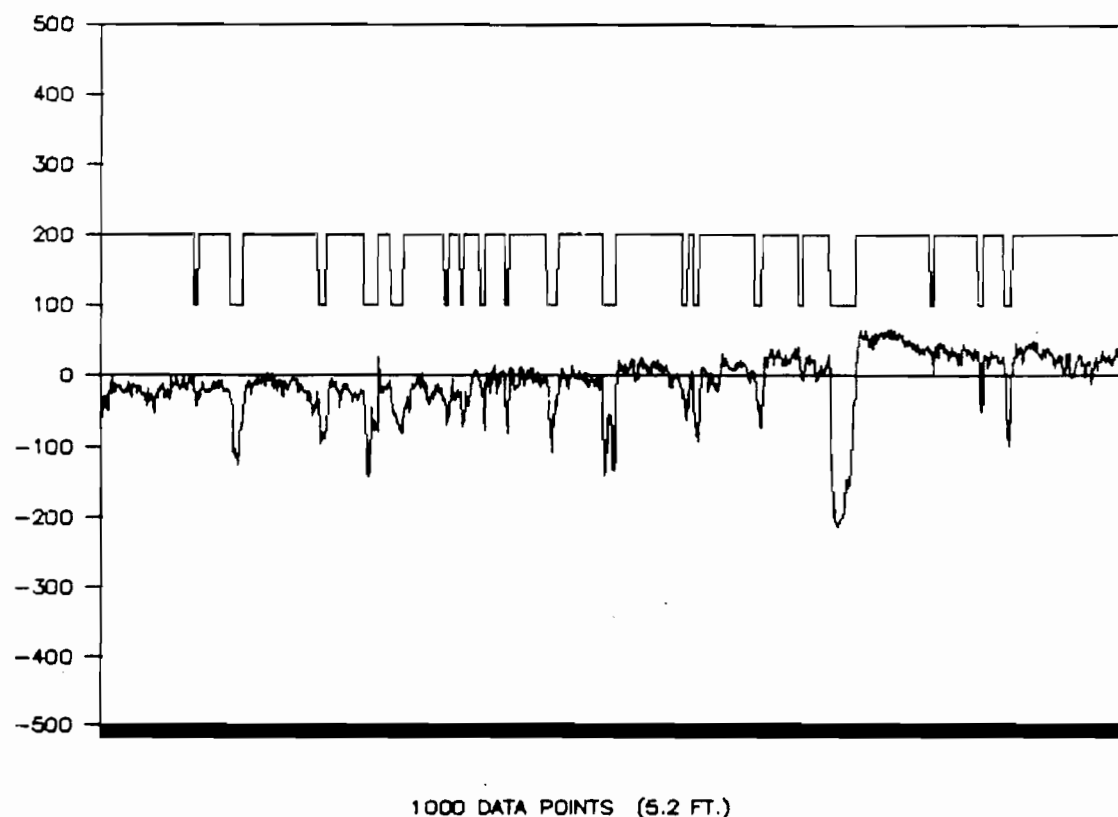


Figure 5.4 Running mean/slope threshold technique applied to severe alligator cracking data

requirement. The autocorrelation difference method is an enhancement of the simple variance method. Using this method the data is first filtered with a highpass filter. Filtering removes the DC component and much of the variability caused by hills, tire bounce, and vehicle suspension effects. This can be seen by comparing the raw data plot in Figure 5.5 with the plot of filtered data in Figure 5.6. With the DC component removed, the data now approximates a zero mean process and the autocorrelation lag 0 is an estimate of the autocovariance lag 0 which, by definition, is the variance.

The autocorrelation difference method involves determining the spread between $r(0)$ and $r(m)$ calculated for every one inch (16 points) block of data. This difference is then compared with a threshold value. As discussed previously, $r(0)$, an estimate of the variance for zero mean data, is large for data with cracking. $r(0)$ will also be large if the data varies too far from the zero mean as is the case on a rough road when the filter is not able to keep the data sufficiently close to a zero mean. This is illustrated in the last 100 data points plotted in Figure 5.6. $r(m)$ is the autocorrelation for data points in the 16 point block which are m time lags apart. $r(m)$, m is typically 4, will decrease more rapidly if variance in the data is higher frequency, that is, sharp cracks.

Using the property $r(0) \geq r(m)$ and examining the four cases for relative values of $r(0)$ and $r(m)$ provides justification for this technique.

CASE I: $r(0)$ small and $r(m)$ small implies a small difference and no cracking.

CASE II: $r(0)$ small and $r(m)$ large is not possible by property $r(0) \geq r(m)$.

CASE III: $r(0)$ large and $r(m)$ small implies a large difference and cracking present.

CASE IV: $r(0)$ large and $r(m)$ large implies a small difference and no cracking.

Figure 5.6 shows filtered data with the $r(0)-r(4)$ value plotted over the sixteenth point of each block of data. Also, any difference greater than 1000 is plotted as 1000 so all information could be plotted on a reasonable scale. As can be seen from the plot, a threshold of 200 identifies all cracks except the one at point A on the plot. Here a shortcoming in the algorithm is illustrated. That is, when one 16 point block ends and another begins in the middle of a small crack it may not be detected.

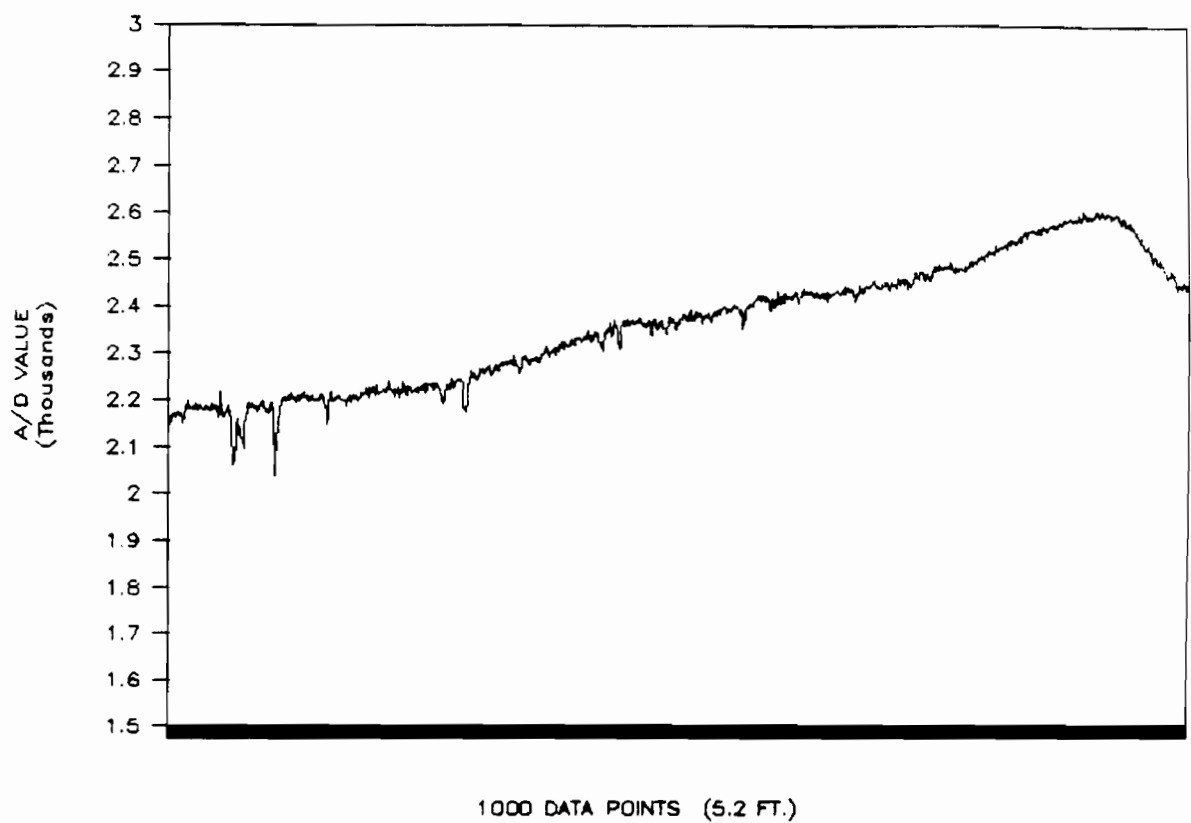


Figure 5.5 Raw data

Figure 5.6 and 5.7 taken together illustrate each of the cases described above. Figure 5.6 shows the difference $r(0) - r(4)$ while Figure 5.7 shows the actual values of $r(0)$ and $r(4)$. For example, Case III was large $r(0)$ and small $r(4)$. The actual values are plotted in Figure 5.7 and then Figure 5.6 can be examined to see the characteristics of the data and the actual difference value.

The autocorrelation difference method has been applied to several of the test sections with good results. In fact, cracking identified by this method compares favorably with that identified by the running mean/slope threshold method. One drawback of this method, however, is that it will not be able to accurately detect crack width.

5.6 AR Process Modeling Results

This technique was investigated to determine whether or not the coefficients obtained by modeling crack data as an AR process could successfully be used to classify cracking types and severity. The assumption was that cracking of the same type and severity would show similar coefficients while the coefficients would be significantly different for a different type and/or severity of cracking.

First, several sections of test data were modeled to determine the number of coefficients to use. It was found that only the first three coefficients contributed significantly; that is, beyond three lags the coefficients were essentially zero. This was also substantiated by the fact that the variance of the white noise, the error term, could only be decreased to a certain level by adding AR terms; beyond that, it really did not improve the model by adding additional terms.

Having determined that three terms should be used in the model, different types of cracking were then examined. Blocks of data one foot in length were examined. It was found that data with more cracking showed higher autocorrelation values and the coefficients were significantly larger than data with no cracking. However, the resolution required to provide the detailed information needed simply was not there. This technique could tell if there was a large amount of cracking or little to no cracking in each one foot block, but that was all. Since the details, such as approximate number of cracks or severity, could not be ascertained, this method was not considered further.

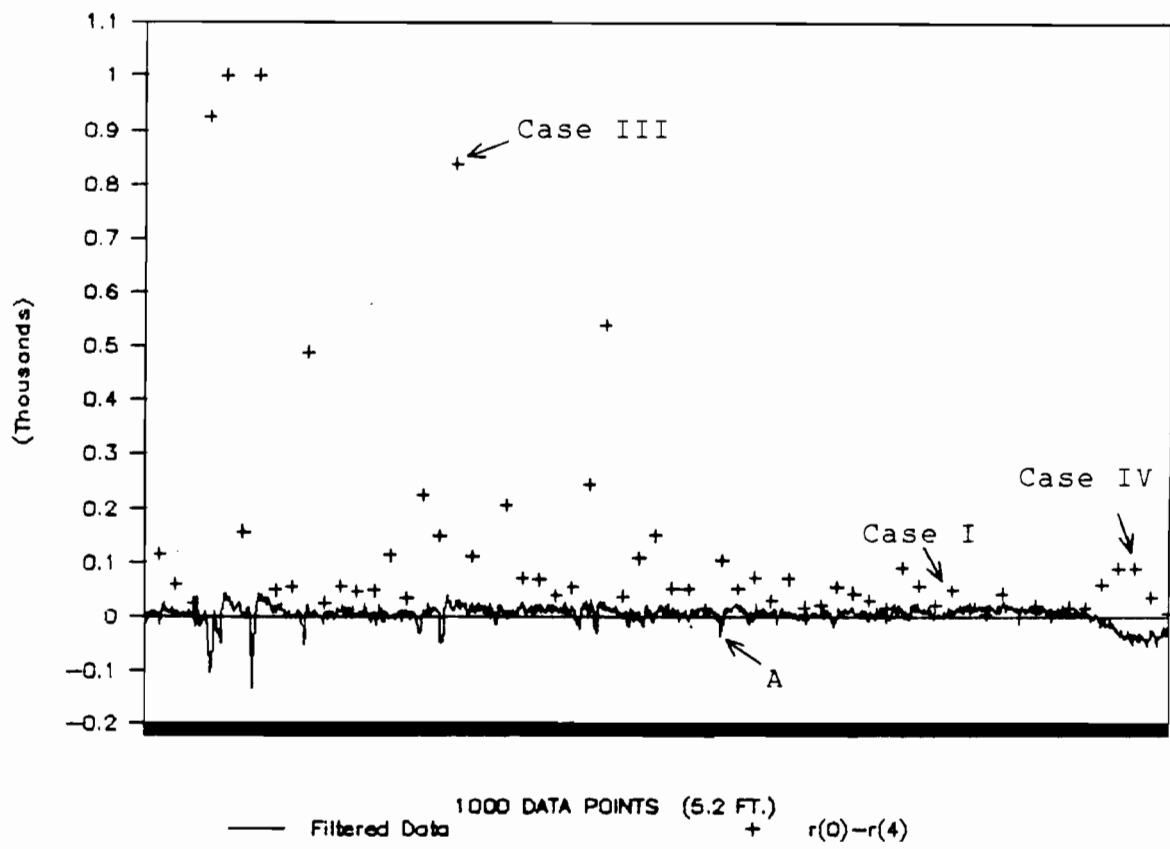


Figure 5.6 Filtered data with $r(0)-r(4)$ value plotted every 16 data points

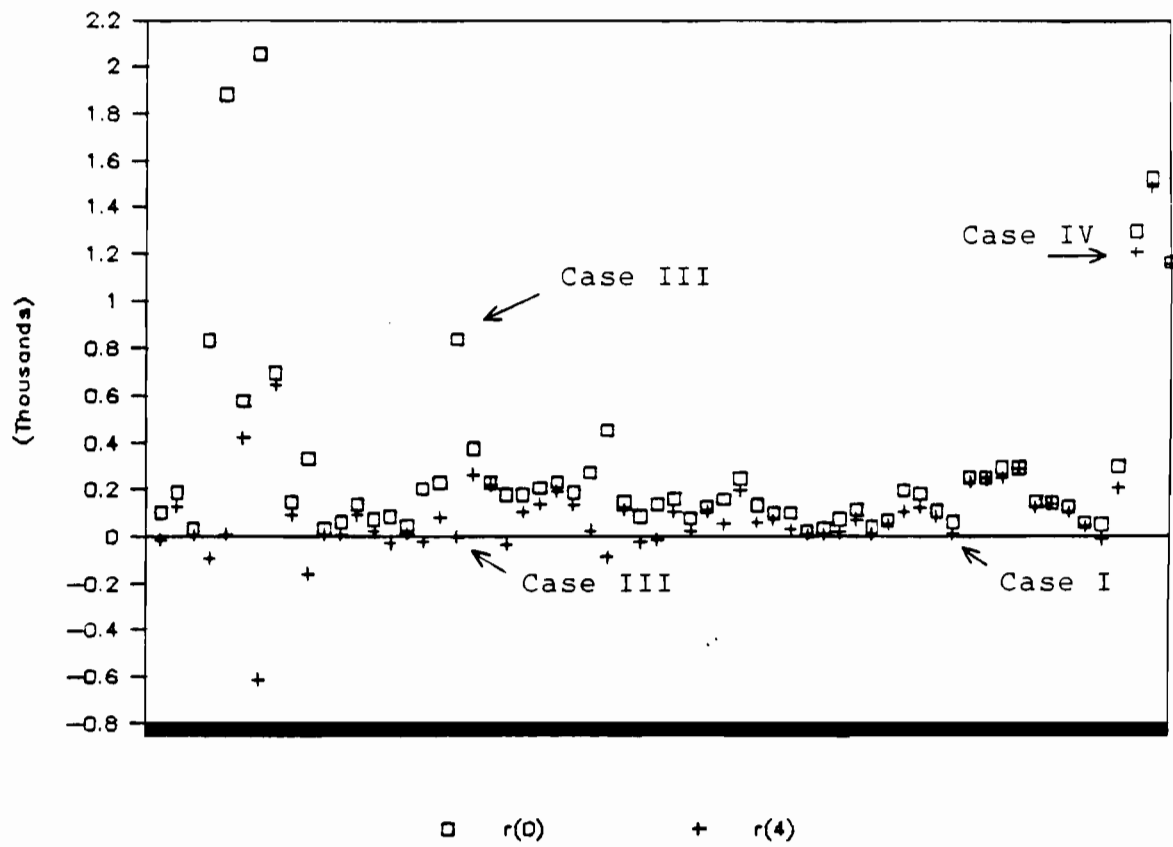


Figure 5.7 Actual $r(0)$ and $r(4)$ values for the data in Figure 5.6

CHAPTER VI

CONCLUSIONS AND FURTHER RESEARCH

The report describes the first two phases of research Project 8-18-86-1141 for developing an automated method of obtaining and evaluating pavement distress and cracking information for PES. For these initial two phases, the use of two lasers, one in each wheel path, are used to obtain cracking data which is processed on a Motorola 68000 based data acquisition board and the COMPAQ Portable III. For detailed analysis, the data is filtered to remove the DC component and long wavelengths before processing. The data is analyzed using several different statistical techniques. Two techniques in particular have been shown to be very reliable. These are the running mean/slope threshold and the autocorrelation difference methods. Software still needs to be written which take the results from these two methods and provide the detailed reporting, that is, the percentage and severity of each cracking type within the section.

Several important conclusions can be made as a result of this initial study. First, alligator and block pavement cracking can be detected using the Selcom lasers mounted in the wheel paths. However, it is unlikely that transverse cracking can be accurately identified. It is believed that additional lasers must be installed to obtain data across the lane before the system will be able to provide this information. Using only two lasers it is simply too likely that something in 30 to 50 feet of data will appear to be a crack even on smooth pavement. With multiple lasers, transverse cracking would be identified only after each laser across the lane had detected a crack within the same foot or two of data. It should perhaps be pointed out that multiple lasers would also allow rutting to be detected. Recall, rutting is one of the seven distress types currently reported by PES. Three lasers are being investigated in Phase 3.

Another issue which remains unresolved is whether or not slight (less than 1/8 inch) cracking is accurately detected. The old lasers with 3/8 by 1/8 inch spot size could not detect them. The new lasers with 1/4 by 1/16 inch spot size have performed reasonably well on the laser calibration board but have not been thoroughly field tested due to the forementioned problems.

Any user of this system must understand the limitations imposed by trying to detect cracking using only two narrow beams of laser light running parallel to the centerline. Obviously, massive amounts of information across the lane is not available. Due to the nature of the sensors used, cracks detected in failures and longitudinal cracking patterns will be misclassified as alligator or block cracking. There is little that can be done to prevent this using lasers as sensing devices. The distress types such as failures, patching and longitudinal cracking can only be detected if the entire lane is examined using video cameras as described by other researchers [6,7]. Video system provide much more detail, but this extra detail presents problems in processing out the unwanted information. A system with a small cluster of lasers along and in between each wheel path would seem to provide the best choice, however, would likely be to costly.

As pointed out numerous times, the algorithms developed for detailed identification and analysis cannot be performed in real-time with the hardware developed in this initial study. Prototype boards which are wirewrapped, such as the DAQ board built for this project, are limited to clock speeds less than 10 MHz because of noise problems, regardless of the maximum clock frequency allowed. Therefore, to obtain faster speeds, printed circuit boards must either be built or purchased. Also, to obtain more computing power a 32-bit microprocessor should be considered over the 16-bit 68000.

It is believed the open architecture VMEsystem developed by Motorola should provide needed hardware upgrades for this project. The VMEsystem allows the user to purchase a basic cardcage which has the VMEbus interconnect standard. The user can then configure the system for his specific needs by purchasing individual VMEmodules which simply plug into the VMEbus with the widely accepted eurocard connector. Typical VMEmodules are microprocessor boards, memory boards, various controller boards, and I/O boards. The VMEsystem architecture allows the user to configure a multiprocessor system with both local and shared memory.

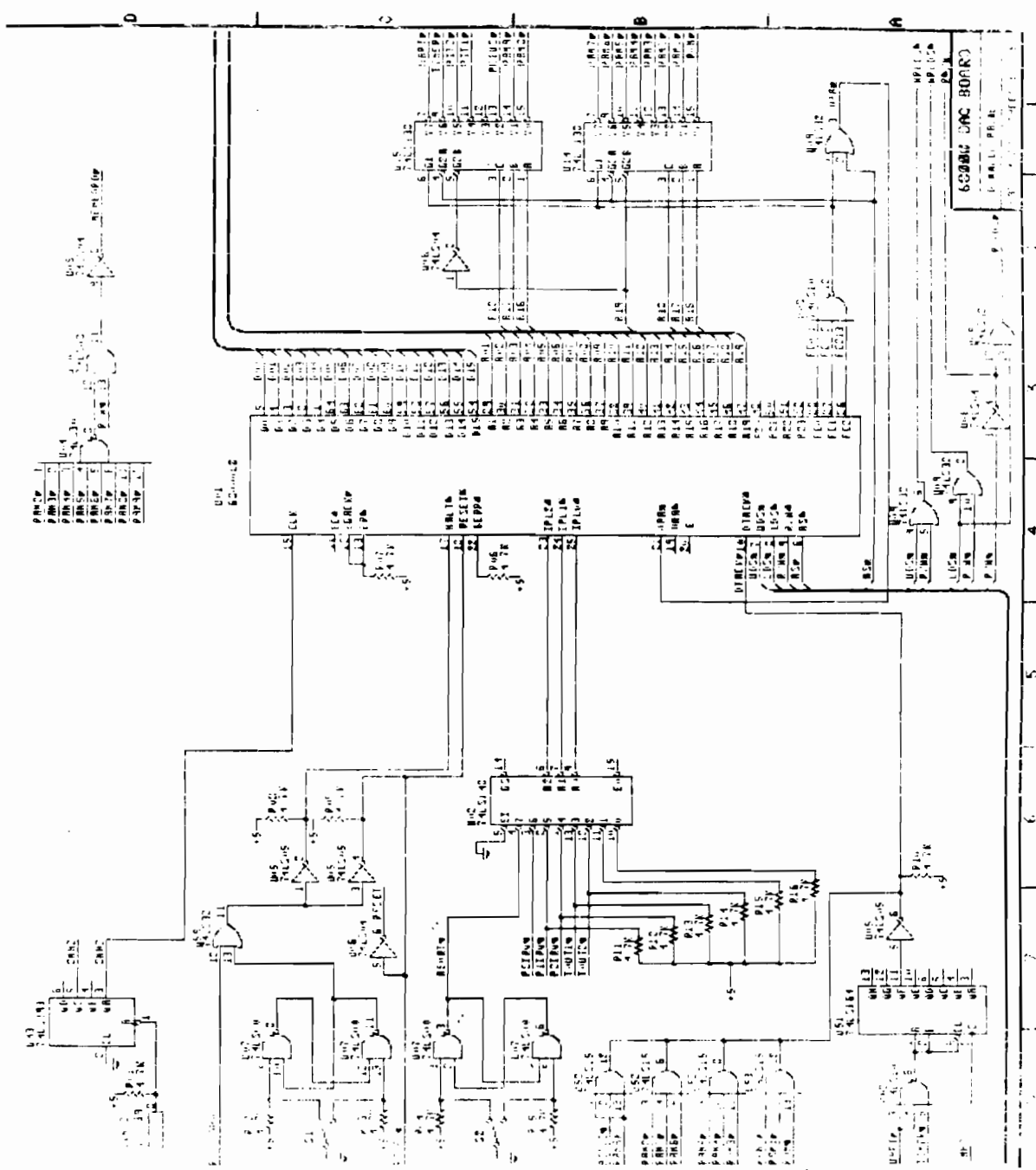
A multiprocessor VMEsystem is currently being assembled for this project. For this system VMEmodules with the 68020 microprocessor interface to the PC. Each of these VMEmodules will be dedicated to processing the data from a single laser. This system should provide the computing power needed to filter the data and identify cracking, at least with the autocorrelation difference method, in real-time.

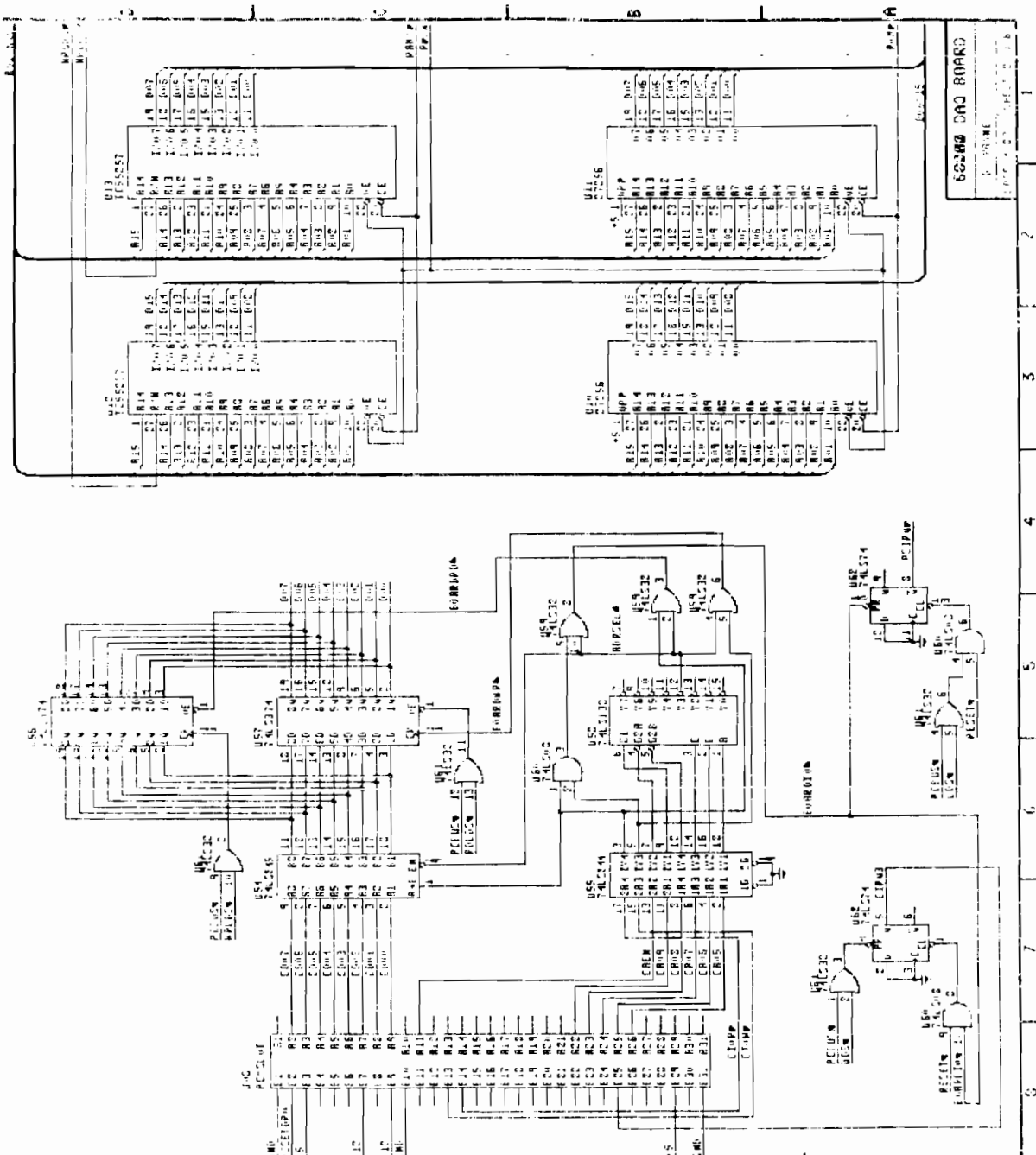
It is still questionable whether or not the running mean/slope threshold method, which provides severity information, will run in real-time. It may very well be the case that the data will be filtered and cracks identified in

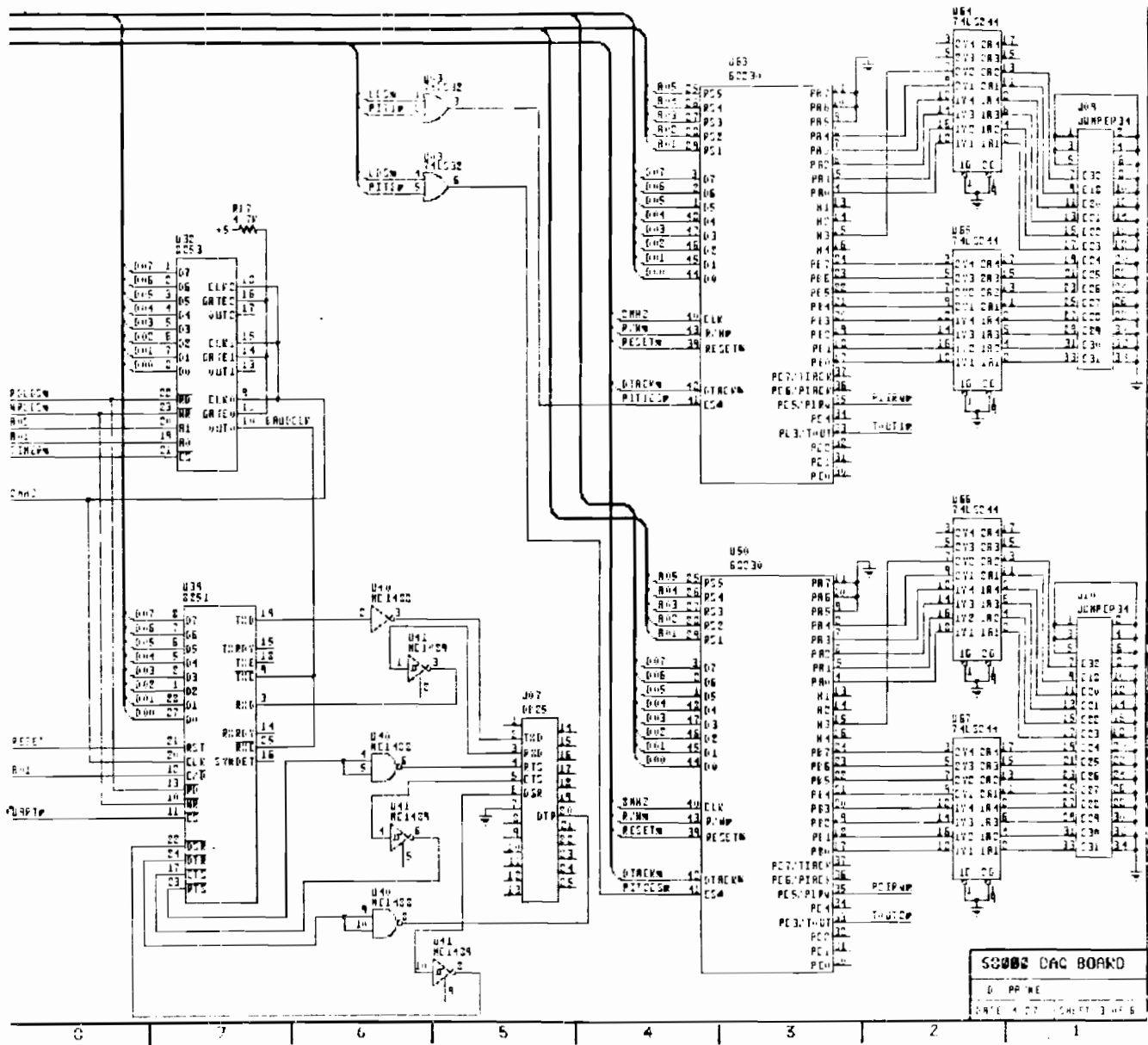
real-time but severity information obtained off-line from a reduced data set stored on the COMPAQ. If a reduced data set is required, data compression techniques will need to be investigated further.

Several other methods are yet to be investigated, which may aid in identifying cracks. Once specific algorithms have been identified, the generality of the 68020 microprocessors may not be required and a system using special purpose signal processing chips may be possible.

APPENDIX A
DAQ BOARD SCHEMATICS

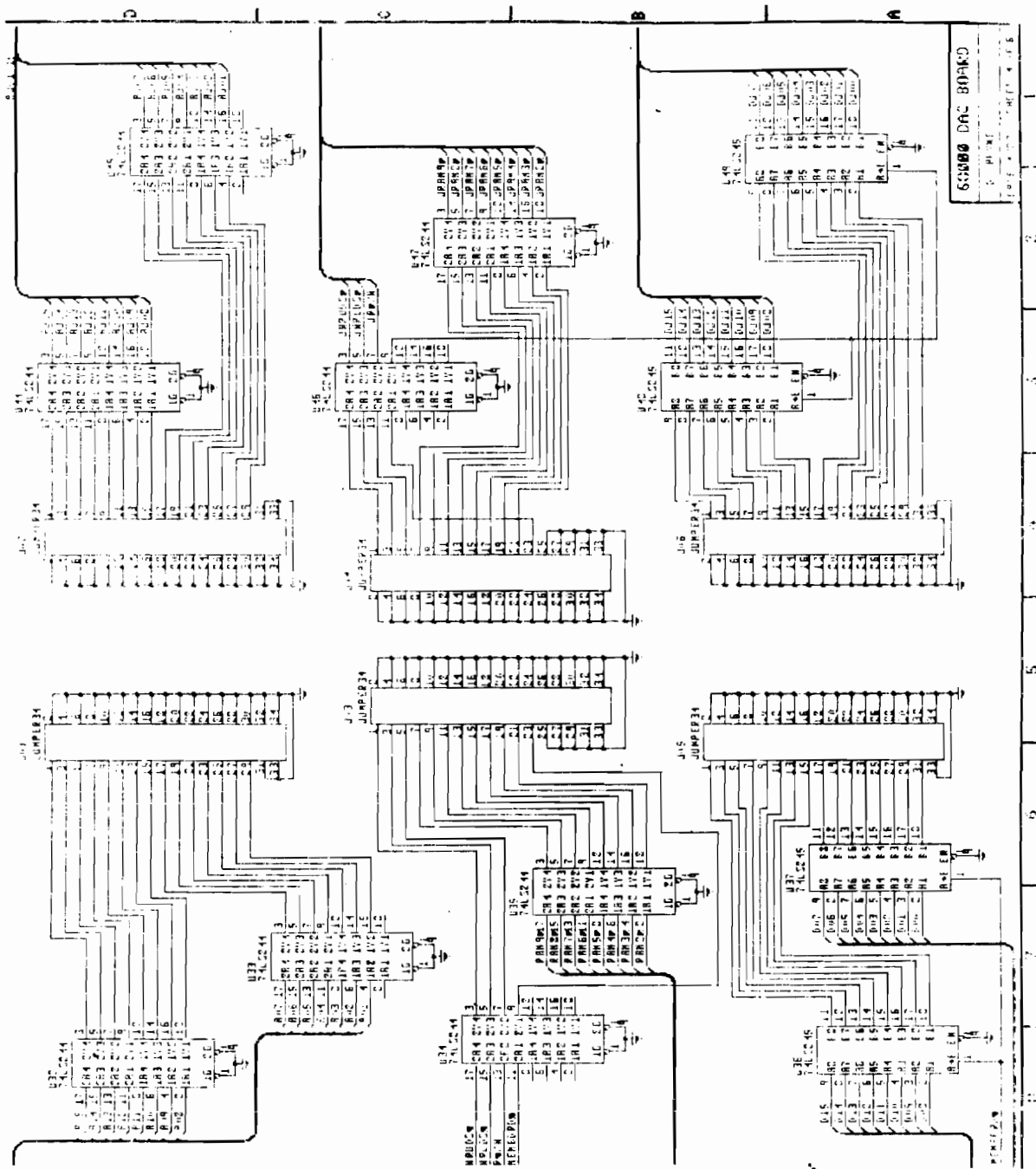


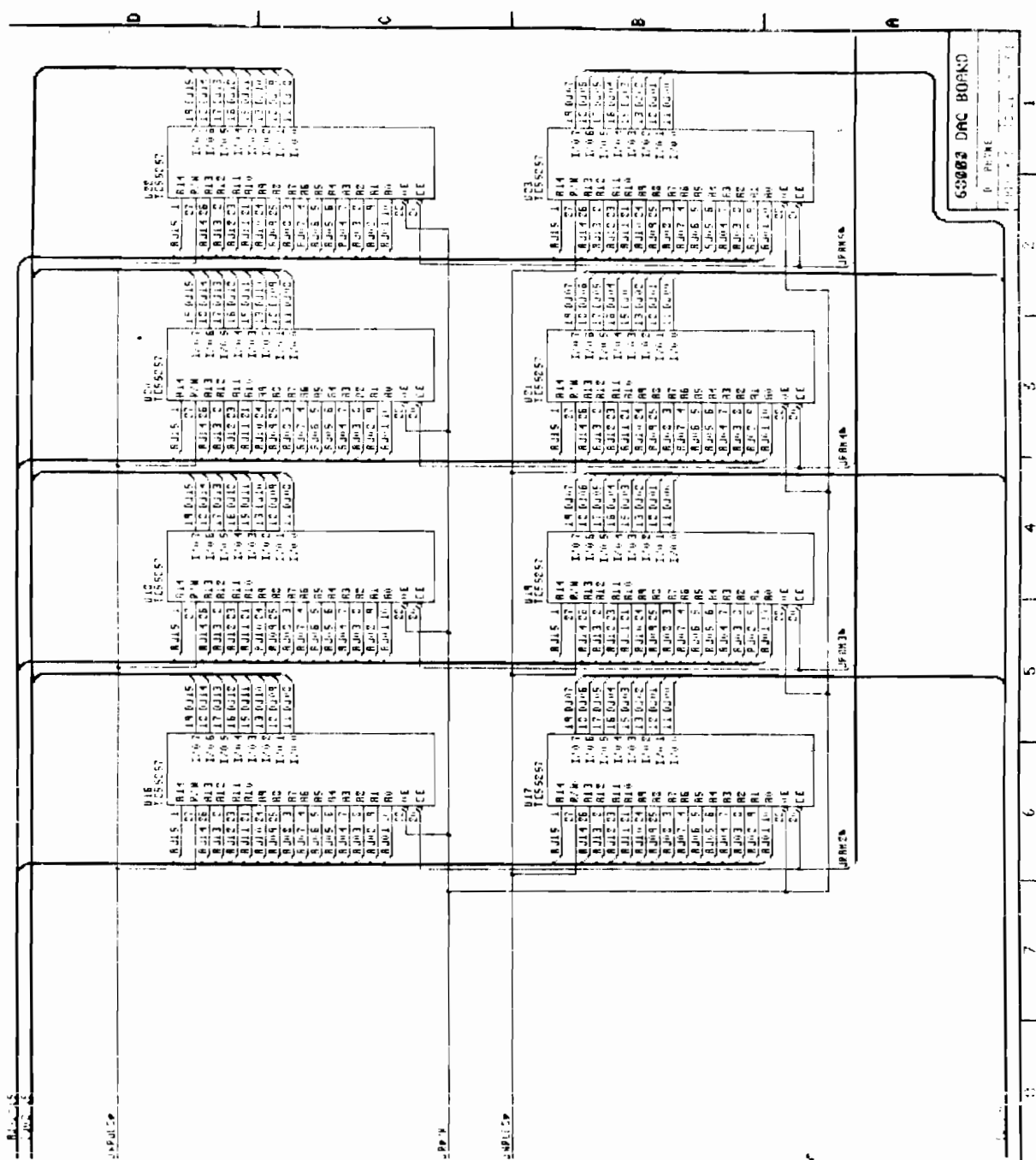


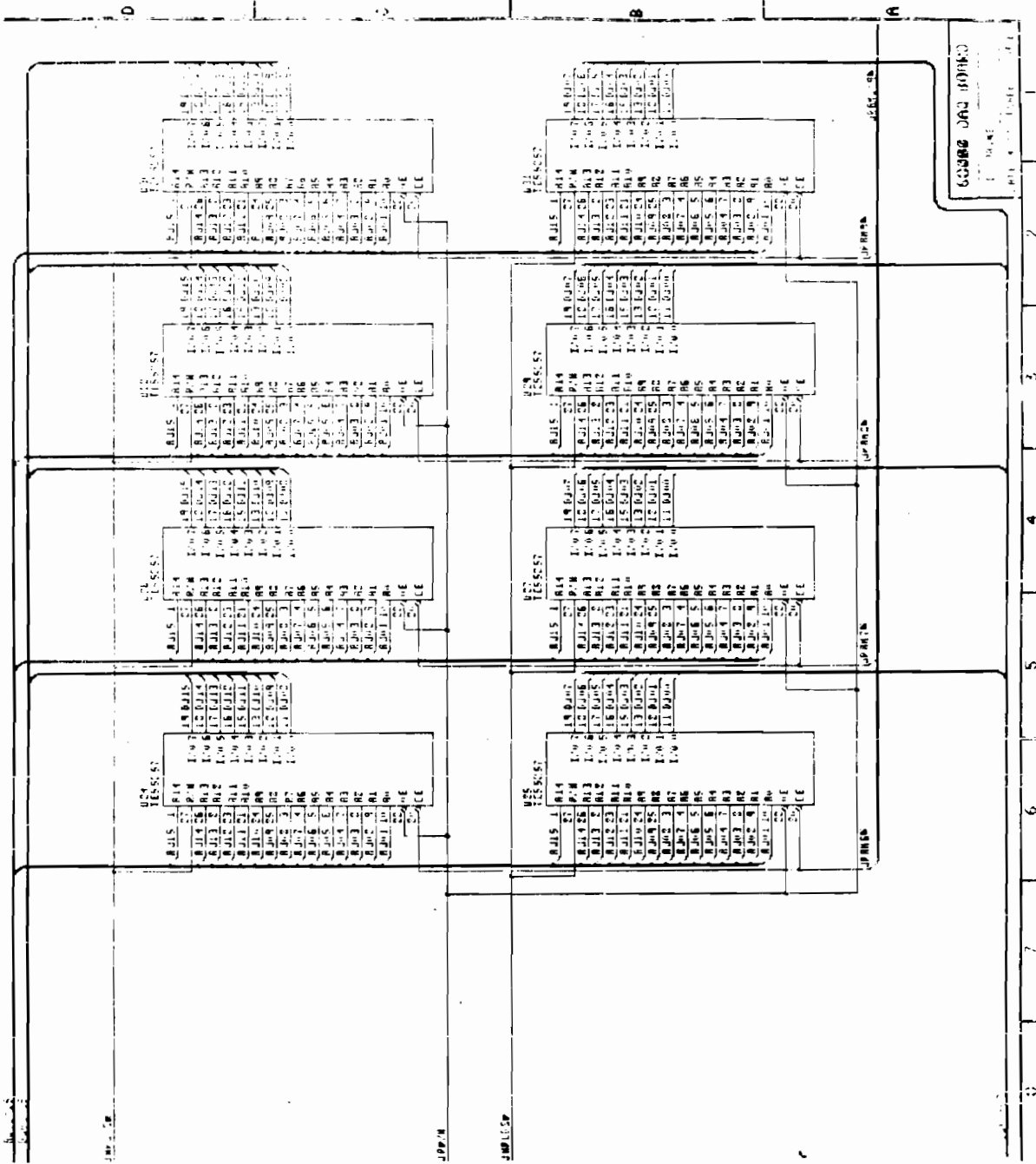


SCOPE CAC BOARD

D PPTME







APPENDIX B
RUNNING MEAN/SLOPE THRESHOLD LISTING

```

C*****
C
C      This program inputs a filtered data file and
C      detects cracks using the running mean/slope
C      threshold method described in Chapter V.
C
C
C      FILEIN - input data file
C      FILEOUT - output file containing crack info
C                  for plotting
C      XM - array of X values used in current mean
C      XD - array of X values used in lookahead if
C              values are decreasing
C      XU - array of X values used in lookahead if
C              values are increasing
C      M - pointer into XM array
C      D - down counter
C      U - up counter
C      DX - value output to file for plotting cracks
C              200 = ground level
C              300 = above gnd level (spikes or errors)
C              100 = crack
C      C - counter of number of points in crack
C              if > 96 (6") will reset
C      IC - same as C but above gnd level
C      NPTS - number of data points
C      NPTSXBAR - number of points to use in mean
C      MTHRESH - threshold value
C      NBASE - number of lookahead points
C      XBAR - running mean
C*****
C
C      PROGRAM RMST
C      CHARACTER*24 FILEIN,FILEOUT
C      DIMENSION XM(8),XD(8),XU(8)
C      INTEGER U,D,IC,C
C      WRITE(*,*) 'Input file for detect? '
C      READ(*,901) FILEIN
901   FORMAT(A24)
C      WRITE(*,*) 'Output file for detect? '
C      READ(*,901) FILEOUT
C      WRITE(*,*) 'Number of data points? '
C      READ(*,*) NPTS
C      WRITE(*,*) 'Number of points to use in mean? '
C      READ(*,*) NPTSXBAR
C      WRITE(*,*) 'Mean threshold? '
C      READ(*,*) MTHRESH
C      WRITE(*,*) 'Slope base length? '
C      READ(*,*) NBASE
C      OPEN(UNIT=2,FILE=FILEIN,STATUS='OLD')
C      OPEN(UNIT=3,FILE=FILEOUT,STATUS='NEW')
C
C      Initialize XBAR and XM array

```

```

C
READ(2,*) X
XBAR=X
XTOT=XBAR*NPTSXBAR
DO 30 I=1,NPTSXBAR
    XM(I)=X
30 CONTINUE
M=1
DX=200
WRITE(3,*) DX
L=2
U=0
D=0
IC=0
C=0
C
C      Loop over all points
C
DO 500 K=2,NPTS
    READ(2,*) X
C
C      Check if X going up or down
C
IF(X.LT.XBAR) THEN
C
C      Going down so reset UP counters and arrays
C
IF(U.NE.0) THEN
    IC=0
    C=0
    DO 100 J=1,U
        XTOT=XTOT-XM(M)+XU(J)
        XM(M)=XU(J)
        M=M+1
        IF(M.GT.NPTSXBAR) M=1
        DX=200
        WRITE(3,*) DX
100 CONTINUE
    XBAR=XTOT/NPTSXBAR
    U=0
ENDIF
C
C      Increment DOWN count, store in array and
C      check if surpasses threshold
C
    D=D+1
    XD(D)=X
    IF(XBAR-X.GE.MTHRESH) THEN
        DO 110 J=1,D
            DX=100
            WRITE(3,*) DX
            C=C+1

```

```

110      CONTINUE
C
C      Check if have been in crack too long and
C      RESET if > 6"
C
C          IF(C.GT.96) THEN
C              C=0
C              XBAR=X
C              XTOT=XBAR*NPTSXBAR
C              DO 120 J=1,NPTSXBAR
C                  XM(J)=X
120      CONTINUE
C              M=1
C          ENDIF
C          D=0
C      ELSE
C
C          If were decreasing for NBASE number of
C          of lookahead points but did not surpass
C          threshold then update by 1 point and cont.
C
C          IF(D.EQ.NBASE) THEN
C              IC=0
C              C=0
C              XTOT=XTOT-XM(M)+XD(1)
C              XBAR=XTOT/NPTSXBAR
C              XM(M)=XD(1)
C              M=M+1
C              IF(M.GT.NPTSXBAR) M=1
C              DX=200
C              WRITE(3,*) DX
C              DO 130 J=1,NBASE-1
C                  XD(J)=XD(J+1)
130      CONTINUE
C              D=NBASE-1
C          ENDIF
C      ENDIF
C*****
C
C      Similar code as for DOWN but here are going
C      UP
C*****
C
C      ELSE
C          IF(D.NE.0) THEN
C              IC=0
C              C=0
C              DO 200 J=1,D
C                  XTOT=XTOT-XM(M)+XD(J)
C                  XM(M)=XD(J)
C                  M=M+1
C                  IF(M.GT.NPTSXBAR) M=1

```

```

        DX=200
        WRITE(3,*) DX
200    CONTINUE
C      XBAR=XTOT/NPTSXBAR
        D=0
ENDIF
U=U+1
XU(U)=X
C
C      Make X surpass 3*threshold before kick out as
C      data point not to be included in running mean
C
        IF(X-XBAR.GE.3*MTHRESH) THEN
          DO 210 J=1,U
            DX=300
            WRITE(3,*) DX
            IC=IC+1
210      CONTINUE
C
C      Checking if need to reset
C
          IF(IC.GT.96) THEN
            IC=0
            XBAR=X
            XTOT=XBAR*NPTSXBAR
            DO 220 J=1,NPTSXBAR
              XM(J)=X
220      CONTINUE
            M=1
          ENDIF
          U=0
        ELSE
          IF(U.EQ.NBASE) THEN
            IC=0
            C=0
            XTOT=XTOT-XM(M)+XU(1)
            XBAR=XTOT/NPTSXBAR
            XM(M)=XU(1)
            M=M+1
            IF(M.GT.NPTSXBAR) M=1
            DX=200
            WRITE(3,*) DX
            DO 230 J=1,NBASE-1
              XU(J)=XU(J+1)
230      CONTINUE
            U=NBASE-1
          ENDIF
        ENDIF
500    CONTINUE
C
C      Through all data points, account for any

```

```
C      data points left in UP or DOWN arrays
C
IF (U.GT.0) THEN
  DO 600 I=1,U
    DX=200
    WRITE(3,*) DX
600  CONTINUE
ENDIF
IF (D.GT.0) THEN
  DO 700 I=1,D
    DX=200
    WRITE(3,*) DX
700  CONTINUE
ENDIF
STOP
END
```

REFERENCES

- [1] Walker, Roger S., Freddy L. Roberts, and W. Ronald Hudson, "A Profile Measuring, Recording, and Processing System", Research Report 73-2, Center for Highway Research, The University of Texas at Austin, April 1970.
- [2] Claros, German J., W. Ronald Hudson, and Clyde E. Lee, "Performance of the Analog and the Digital Profilometer with Wheels and with Non-Contact Transducers", Research Report 251-3F, Center for Highway Research, Bureau of Engineering Research, The University of Texas at Austin, April 1985.
- [3] Walker, Roger S., and John Stephen Schuchman, "Upgrade of 690D Surface Dynamics Profilometer for Non-Contact Measurements", Research Report 494-1F, The University of Texas at Arlington, December 1986.
- [4] "Selcom Technical Manual", Selective Electronic Co., (unpublished).
- [5] "Selcom User's Manual", Selective Electronic Co., (unpublished).
- [6] Cox, Gregory M., Donald Fronek, and Rahn Merrill, "Real-time Computer Vision Using Intelligent Hardware", Applications of Artificial Intelligence III, SPIE vol. 635, pp. 564-574, 1986.
- [7] Mahler, David S., "Final Design of Automated Pavement Crack Measurement Instrumentation from a Survey Vehicle", Report No. FHWA/RD-85/077, Federal Highway Administration, Washington, D.C., 1985.
- [8] "Pavement Evaluation System Rater's Manual", Texas State Department of Highways and Public Transportation, 1987.

- [9] Epps, J. A., A. H. Meyer, I. E. Lattimore, Jr., and H. L. Jones, "Roadway Maintenance Evaluation User's Manual", Research Report 151-2, Texas Transportation Institute, Texas A&M University, September 1974.
- [10] Smith, Roger E., Michael I. Darter, and Stanley M. Herrin, "Highway Pavement Distress Identification Manual for Highway Condition and Quality of Highway Construction Survey", Federal Highway Administration, Washington, D.C., 1979.
- [11] Box, George E. P., and Gwilym M. Jenkins, Time Series Analysis: Forecasting and Control, Holden-Day Inc., San Francisco, California, 1976.
- [12] Jenkins, Gwilym M., and Donald G. Watts, Spectral Analysis and Its Applications, Holden-Day, Inc., San Francisco, California, 1968.
- [13] Papoulis, Athanasios, Probability, Random Variables, and Stochastic Processes, McGraw-Hill, Inc., New York, 1984.
- [14] Oppenheim, Alan V., and Ronald W. Schafer, Digital Signal Processing, Prentice-Hall, Inc., Englewood Cliffs, New Jersey, 1975.
- [15] Childers, Donald G., ed., Modern Spectral Analysis, IEEE Press, New York, 1978.
- [16] Cooley, J. W., and J. W. Tukey, "An Algorithm for the Machine Calculation of Complex Fourier Series", Math. Comput., vol. 19, pp. 297-301, April 1965.
- [17] Welch, Peter D., "The Use of Fast Fourier Transform for the Estimation of Power Spectra: A Method Based on Time Averaging Over Short, Modified Periodograms", IEEE Trans. Audio and Electroacoust., vol. AU-15, pp. 70-73, June 1967.
- [18] Ahmed, Nasir, and T. Natarajan, Discrete-Time Signals and Systems, Reston Publishing Company, Inc., Reston, Virginia, 1983.

- [19] Digital Signal Processing Committee, ed., Programs for Digital Signal Processing, IEEE Press, New York, 1979.
- [20] Koopmans, L. H., The Spectral Analysis of Time Series, Academic Press, New York, 1974.
- [21] Graupe, Daniel, Time Series Analysis, Identification and Adaptive Filtering, Robert E. Krieger Publishing Co., Malabar, Florida, 1984.
- [22] Marple, S. Lawrence, Jr., Digital Spectral Analysis With Applications, Prentice-Hall, Inc., Englewood Cliffs, New Jersey, 1987.
- [23] Clements, Alan, Microprocessor Systems Design: 68000 Hardware, Software, and Interfacing, PWS Publishers, Boston, Massachusetts, 1987.
- [24] Coffron, James William, Using and Troubleshooting the MC68000, Reston Publishing Company, Inc., Reston, Virginia, 1983.
- [25] Eggebrecht, Lewis C., Interfacing to the IBM Personal Computer, Howard W. Sams and Co., Inc., Indianapolis, Indiana, 1983.
- [26] MC68000 : 16-/32-Bit Microprocessor, Motorola Semiconductors, Austin, Texas, 1985.
- [27] MC68230 : Parallel Interface/Timer (PI/T), Motorola Semiconductors, Austin, Texas, 1983.
- [28] The TTL Data Book, Vol. 2, Texas Instruments Inc., Dallas, Texas, 1985.
- [29] Uffenbeck, John, The 8086/8088 Family : Design, Programming, and Interfacing, Prentice-Hall, Inc., Englewood Cliffs, New Jersey, 1987.

- [30] Wilcox, Alan D., 68000 Microcomputer Systems: Design and Troubleshooting, Prentice-Hall, Inc., Englewood Cliffs, New Jersey, 1987.
- [31] Durbin, J., "The Fitting of Time Series Models", Rev. Inst. Int. de Stat., vol. 28, pp. 233-244, 1960.
- [32] Levinson, N., "The Weiner (Root Mean Square) Error Criterion in Filter Design and Prediction", J. Math. Phys., vol. 25, pp. 261-278, 1947.